RESEARCH CENTRE FOR MODELING AND SIMULATION (RCMS)

DRAG REDUCTION IN SUPERSONIC BLUNT BODIES USING OPPOSING JETS

ATIQA BIBI

NATIONAL UNIVERSITY OF SCIENCES AND TECHNOLOGY (NUST), ISLAMABAD

2016

DRAG REDUCTION IN SUPERSONIC BLUNT BODIES USING OPPOSING JETS

ATIQA BIBI

Research Centre for Modeling and Simulation

A thesis submitted to the National University of Sciences & Technology

in partial fulfillment of the requirement for the degree of

Masters of Science

2016

STATEMENT OF ORIGINALITY

I hereby certify that the work embodied in this thesis is the result of original research and has not been submitted for a higher degree to any other University or Institution.

Date	Atiqa Bibi

Dedication

This effort is dedicated to all those humble beings that have assisted me in any way to become what I am today, whose sacrifices seeded my success, especially my parents who have felt my pain beyond me and showered me with never ending prayers and support. I deem them as a divine source of inspiration.

Acknowledgements

All praise to Allah Almighty for bestowing me with the courage, knowledge and health to carry out this thesis.

I am greatly indebted to my Parents and family members, without their endless support, patience and prayers the very idea of this study was impossible.

I would like to pay my humble gratitude to PMO, NESCOM for providing me the time and resources to complete my higher studies.

I sincerely appreciate the continuous motivation of my project advisor Dr. Adnan Maqsood and Co-Supervisor Dr. Salma Sherbaz. Their encouragement was the main source of strength that stimulated me to complete this thesis.

I would specially like to extend a heartfelt thanks to my thesis committee members Dr. Majid Ali (CES) and Dr. Ammar Mushtaq (RCMS) for their precious time and skillful assistance.

I am also grateful for the computing facilities provided to me by Super Computing Lab, RCMS, NUST Islamabad, without them I would never be able to run such an extensive computational analysis.

Summary

Typical objectives of commercial aeronautics research during twentieth century were centered on achieving long range, high altitude and speed. However, the speed of commercial aviation was curtailed to subsonic and transonic flow regimes. Efforts in the form of Concorde and Tupolev-144 were made for supersonic commercial travels but economic viability and safety concerns with supersonic commercial vehicles have pushed the humanity back to transonic regime.

One peculiar design feature of supersonic wings, fuselage nose and atmospheric entry vehicles is blunt-shaped leading edge/nose commonly referred as blunt bodies. It is an important research area for gas dynamists. The main motivation of this research is to understand the complex shock wave pattern formed ahead of the blunt bodies and alleviate its adverse contributions that are high drag, high acoustic signature and high aerodynamic heating.

In this study, a number of flow control methods have been used to manipulate flow fields for drag reduction. These methods have been broadly classified under two group's namely active and passive techniques. Among the active flow control techniques, the opposing jet method has gained immense popularity in the research community. It consists of ejection of jet from stagnation point of a blunt body in the upstream direction. The free stream fluid then turns this jet to flow in the rearward direction forming a shear layer over the body surface, thus protecting it from high pressure and high temperature external environment. In this thesis, a numerical study is conducted to observe the effects of simple jet as well as jet emanating from divergent nozzle located at the nose of a blunt hemispherical body. Numerical data is

duly validated with experimental results. Extensive numerical simulations are conducted by varying both length and angle of divergent nozzle. The results show a considerable reduction in drag by the use of a divergent nozzle. Specifically, 46 % and 56% reduction in drag coefficient is achieved at pressure ratio of 0.6 and 0.8 respectively in the divergent nozzle cases as compared to the simple blunt body without any nozzle.

Table of Contents

List of Figures

List of Tables

CHAPTER 1

Introduction

1.1 Background

By the end of world war II supersonic flight gained great importance in the form of high speed rockets. The development of Inter-Continental Ballistic Missiles (ICBM) started in 1953 [1]. From here began an era of supersonic vehicles which through further advancement have evolved into hypersonic travelers including jet aircrafts, missiles, space shuttles and re-entry vehicles. All these missions must combat a common feature of high drag, high temperature environment and high acoustic signature. Therefore, with the development of supersonic travelers in the early 1950's; efforts to combat their severe aerodynamic environments were also initiated alongside.

1.2 Flow Control Technologies

A pertinent area of research in fluid mechanics is the control of fluid flow field to achieve desired results. Fluid flow control may involve efforts to enhance, delay or suppress phenomenon such as transition, separation and turbulence. This can improve mixing, heat transfer, lift and drag profiles. Flow manipulation of a system can contribute to its overall efficiency, maneuverability, economy and reusability. The flow control technologies have been classified under two major groups

- Passive methods
- Active methods

1.2.1 Passive Flow Control Methods

Passive methods involve flow control by using techniques which do not introduce any energy or power to the flow. Flow is usually manipulated by using

different geometric shapes as per application requirement. Various methods are used for separation control or drag reduction including grooves, ribs, spikes and their combination [2]. Among these techniques the mechanical spike has gained most importance. The spike is a thin cylindrical rod of fixed length mounted at the stagnation point of the blunt body [3]. It modifies fore body flow field in two ways. Firstly, it breaks the single strong shockwave into a series of weak oblique shock waves. Secondly, it causes flow separation and creates a shear layer which reattaches downstream of fore body region [3] as shown in Figure 1-1. A comprehensive review of the spike technology was done by Ahmed [4] . A major disadvantage of the mechanical spike is that it requires frequent replacement or continuous cooling as a result of bearing high temperatures during flight.

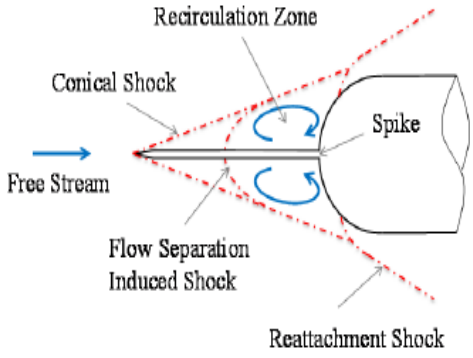

Figure 1-1 Mechanical spike [5]

1.2.2 Active Flow Control Methods

Active flow control technologies introduce energy or power into the flow. This involves techniques such as energy deposition upstream of body, and the use of opposing jets. Energy deposition upstream of the body can help to reduce drag [6]. Figure 1-2 shows the change in flow due to energy deposition. Issues of practical implementation of this method have hindered its advancement. Detailed research on energy deposition method was done by Knight [7].

The opposing jet concept has gained the most interest in the research community due to its reusability and relatively economic implementation as compared to other methods. This method consists of ejection of jet from stagnation point of a blunt body in the upstream direction. The free stream fluid then turns this jet to flow in the rearward direction forming a shear layer over the body surface, thus protecting it from the high pressure, high temperature external environment as shown in Figure 1-3 [8].

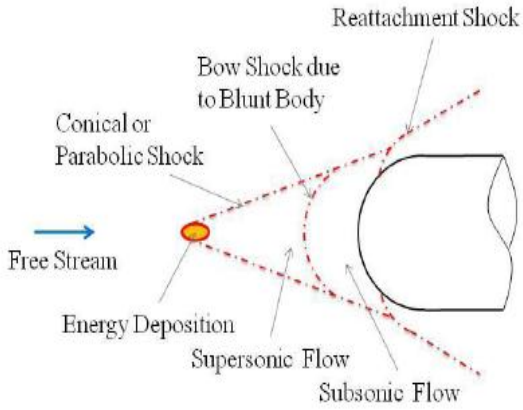

Figure 1-2 Energy Deposition [5]

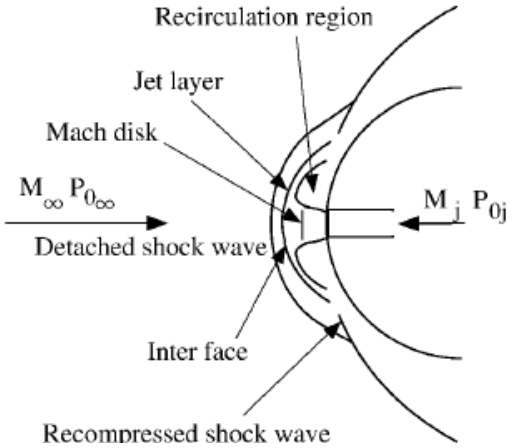

Figure 1-3 Flow Field Due to Opposing Jet [9]

1.3 Area of Research

Although blunt profiles in high speed help in reducing heat transfer to the body, they also increase overall drag experienced by the body. This high value of drag can be useful in re-entry applications where it actually helps to reduce the velocity during re-entry. However, for hypersonic applications where greater velocities are advantageous the blunt body profile produces unnecessary drag. Efforts to reduce drag have been under study since the very inception of high speed vehicles. In this regard, the opposing jet concept has gained the most interest in the research community due to its reusability and relatively economic implementation as compared to other methods. Series of research efforts over the years have showed a marked decrease in both heat and drag experienced by blunt profiles using an opposing jet issuing from the fore body region. All applications whether supersonic, hypersonic and even space exploration systems can achieve more efficient flight missions by the use of counter flowing fore body jets.

Supersonic research activities were initially carried out for military purposes in the form of fighter aircrafts. Besides jets like X-35 and J-31, the supersonic application band also encompasses transport jets like the Concorde, strategic bombers, reconnaissance systems, supersonic cruise missiles like the YJ-91, 3M-54-KLUB and Inter Continental Ballistic Missiles (ICBM). Moreover the remarkable break through into hypersonic flights in the form of aircrafts such as X-15, X-43 and missiles such as Brahmos-II have opened a new gate of research around the globe. The opposing jet can play a key role in overcoming the challenges of the severe flight conditions experienced in these rapidly advancing technologies.

Tremendous efforts have been performed for space exploration over the past sixty years. Space shuttles and re-entry vehicles have reached Mars and beyond. The

new space era is rapidly advancing for the development of many emerging technologies such as Reusable launch vehicles, Orbital transfer vehicles, and the more commercial application of space tourism. The concept underlying RLV's is that instead of expelling a vehicle launched into space after only a single use; it should be reused after servicing. The reusable launch concept has been applied to Single Stage To Orbit (SSTO) vehicles and Two Stage To Orbit (TSTO) vehicles. SSTO vehicles reach orbit from the surface of a body in one stage without expelling any hardware. The Douglas Delta Clipper DC-X and Space Ship One are examples of developing SSTO vehicles, shown in Figure 1-4.

Figure 1-4 (a) The Douglas Delta Clipper DC-X[10] (b) Space Ship One [11]

TSTO vehicles reach orbit velocity in two stages. The reusable launch concepts are also being applied to TSTO. The initial stage should carry the second stage to a certain point, after which it should return back for re-launch purposes. DH-1 shown in Figure 1-5 is an example of a developing TSTO vehicle.

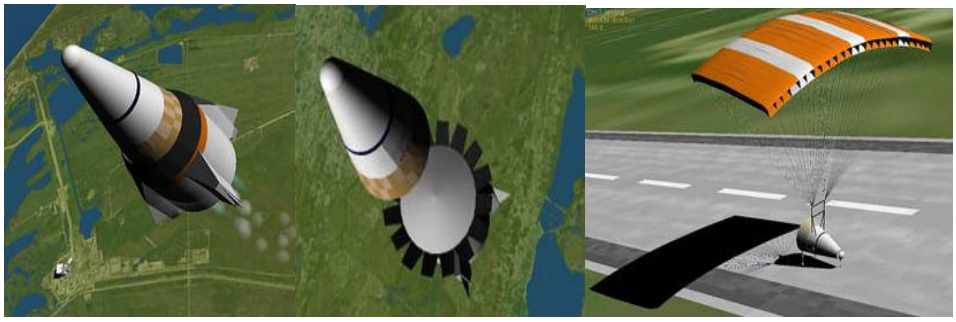

Figure 1-5 DH-1 two stage reusable scheme [12]

Another class of emerging space vehicles is Orbital Transfer Vehicles (OTV) Figure 1-6. These vehicles are intended to perform the function of an intermediate space station between the spacecraft and the ground station. They can be used for resupply of consumables or re-servicing for repair and maintenance purposes [13]. Commercial space flight is another space application gaining interest. Examples of such are the Russian Soyuz spacecraft which has conducted a number of commercial space missions is another manned private space vehicle.

Figure 1-6 Orbital Transfer Vehicles (OTV) [14]

Any vehicle intended to interact with the space environment must be able to overcome the intense heat and drag loads. In the case of reusable launch vehicles, the system should be robust enough to repeatedly withstand these loads. As the forebody region of a space vehicle is the most heavily loaded, it can be protected by counter flowing jets. The number of jets required, their proper placement, jet ejection pressure and material are all adjustments that need to be studied. Advancement in the study of the active flow control system can prove to be quite helpful in progressing research activities for the new space technologies.

1.4 Research Objectives

The objectives of this research endeavor are to:

- Study the effects of jet pressure variations through computational modeling and simulation

- Validate computational results of pressure distribution with experimental data
- Determine drag reduction achieved by opposing jet and divergent nozzle combination s.

1.5 Methodology used for research

The modeling and simulation technique used to analyze the current fluid flow problem will be based on Computational Fluid Dynamics. Two dimensional steady state analyses of a blunt hemispherical body in supersonic flow will be conducted.

This research endeavor will comprise of two phases. In the first phase, jet ejection pressure will be varied to study its effect on drag reduction. The simulated results will be duly validated with experimental data. The base line configuration with available experimental data is selected from the work of Hayashi et al. [15]. In the second phase, combination technique of opposing jet ejected from a diverging nozzle will be studied. A series of geometric iterations by varying both length and angle of divergent nozzle will be conducted. It is anticipated that the current effort will help reach an optimal pressure ratio + nozzle geometry combination that will impart minimum drag to the blunt profile. Figure 1-7 illustrates the research methodology to be adopted.

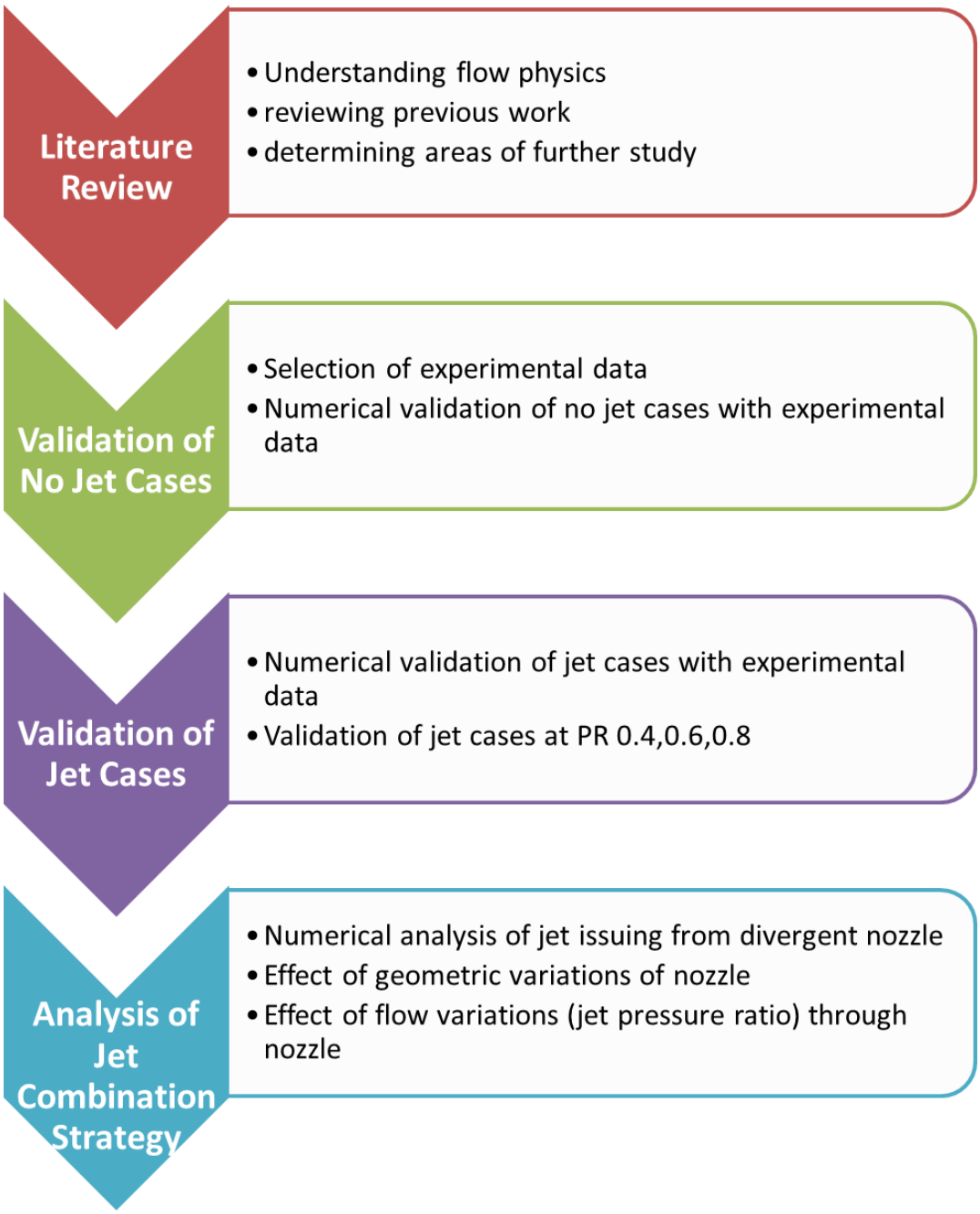

Figure 1-7 Methodology Flow Chart

1.6 Contributions

The opposing jet concept holds significance in a number of application areas. Military requirements of high speed jets as well as robust missiles and the latest space emerging technologies such as reusable launch vehicles and commercial space missions could all benefit immensely from the opposing jet flow control system. The counter flowing jet imparts a significant decrease in the drag and heat loads experienced by a supersonic flyer. This can help to improve the overall economy and efficiency of the mission flight.

1.7 Organization of the Thesis

A brief outline of the chapters included in the present thesis presented below:

Chapter 1 --- Introduction

This chapter gives an introduction of flow control technologies. The area of research together with the formulated research methodology is also outlined. A brief description of the thesis break down is also included.

Chapter 2 --- Literature Review

A detailed review is presented including both international as well as local scope of work. Some of the missing links are also identified.

Chapter 3---Numerical Methodology

In this chapter the numerical procedure adopted for the current analysis is documented in detailed.

Chapter 4 --- Results and Discussion

Results of both the validation cases as well as all the geometric variation cases are presented. A detailed discussion of observed phenomena along with possible reasoning is also mentioned.

Chapter 5 --- Conclusions and Future Work

Conclusions derived from the current research are presented. Recommendations for future efforts are suggested in this chapter.

CHAPTER 2

Literature Review

2.1 Background

A comprehensive summary starting from the seminal work on opposing jet concept to the most recent efforts is presented. The key findings of researchers such as the governing parameters of opposing jet, flow modes (Long Penetration Mode, Short Penetration Mode) are discussed. Relevant work with application to Pakistan is mentioned. Finally, some of the missing links in research efforts are also identified.

2.2 Literature Review

2.2.1 Early Research Efforts

Studies on the use of opposing jet to manipulate flow fields began since early 1950's [16] . Early research in the area was concerned mainly on understanding flow physics of the opposing jet phenomena [17, 18]. The earliest work on heat transfer effects was made by Inouye [19] in which it was concluded that at low flow rates heat transfer to body decreases by the use of opposing jet. A similar conclusion was made by Warren [20] where nitrogen and helium gases were used in opposing jets. It was inferred that as long as the jet flow remains small enough to not penetrate the free stream, heat reduction over body will occur. However, Finley [21] pointed out that Warren's study included very low pressure ratios. Hence, larger pressure ratios beyond the unstable region actually help to reduce heating. This conclusion was also made in the work of Rashis [22].

2.2.2 Experimental Research Efforts

In 1960s and 1970s, attention was directed towards the heat and drag reduction effects of opposing jets. Advancement in the research of opposing jet technology lead to the study of various other aspects such as effect of different jet ejection materials, effect of flow variation and geometric parameters. Warren [20] studied the effect of nitrogen and helium gas on heat transfer rates. Barber [23] studied the effects of hydrogen, helium and nitrogen jets and found the results to significantly vary with jet mass flow rates. From research it has been concluded that the flow field of an opposing jet from a blunt body in supersonic flow mainly depends upon factors such as jet to body diameter ratio, jet to free stream pressure ratio, jet and free stream mach numbers. Initially, Finley [21] studied effect of jet mach no., effect of jet to body diameter ratios, and pressure ratios. Riggins [24] studied the effect of varying exit mach number and exit diameter of jet. His results showed a decrease in drag with decrease in exit Mach number and increase in jet exit diameter Figure 2-1.

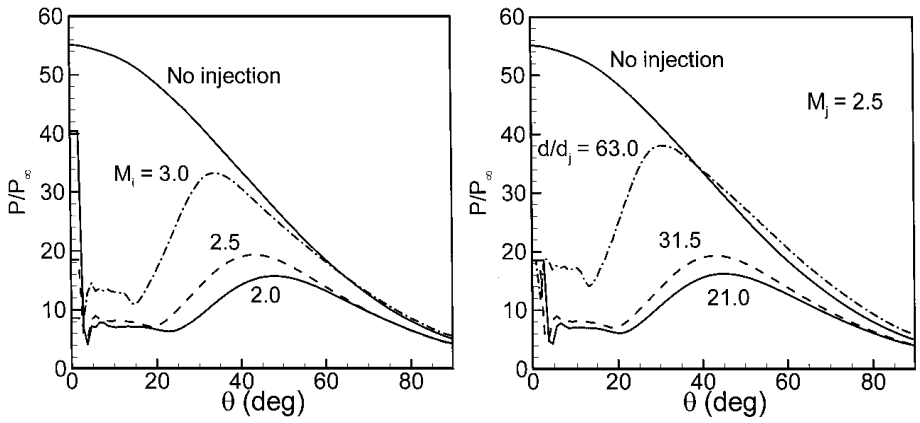

(a) (b)

Figure 2-1 (a) Variation of surface pressure with jet exit mach no. (b) Variation of surface pressure with jet exit diameter [24]

Hayashi [9, 25] experimentally and numerically studied the effect of change in jet exit diameter, temperature, mach number and pressure ratio. He found a decrease in heat loads with increase in pressure ratio, Figure 2-2. Daso *et al.* [16] carried out extensive experimental tests on jet ejection from the nose of blunt reentry body. Effect of changing angle of attack on heat and drag reduction was also catered. In his study, he varied alpha to 9˚ and found that in this range of alpha variation there was not much significant change in flow as compared to alpha 0˚ case.

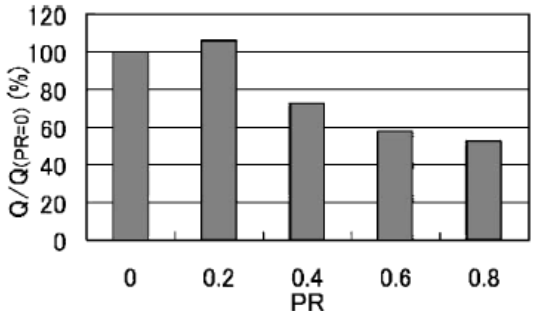

Figure 2-2 Variation of heat loads with jet pressure ratio [9]

Efforts to understand the opposing jet flow phenomena have lead many researchers to identify specific regions of flow [16, 26-28]. Jarvinen and Adams [26] studied different jet penetration modes namely Long Penetration Mode (LPM) and Short Penetration Mode (SPM). They found that LPM occurred at low thrust rates whereas SPM occurred at high thrust rates. Moreover transition from LPM to SPM occurred at a fixed pressure ratio called as the 'critical pressure ratio'. A similar discussion can be found in the works of Hayashi and Zheng [27, 28]. Figure 2-3 indicates difference between long and short penetration modes. Three different regions were identified based on pressure ratio. At small pressure ratios oscillation of shockwave may occur. The shockwave is dispersed and may have long standoff distances from the body. Flow may exhibit diamond shaped patterns. This is known as

unstable region. At higher pressure ratios no oscillations of shockwave occur and shock stand-off distances are lesser. A distinct bow shock and terminal shock can be observed in Figure 2-3(b).There exists a free stagnation point at which both the flows come to rest, and the jet flow reverses its direction towards the body creating a recirculation region. This is known as stable region. There also exists a transition region during which flow changes from unstable to stable region. This region is difficult to capture. Figure 2-4 is an experimentally captured image of transition mode from the works of Daso [16].

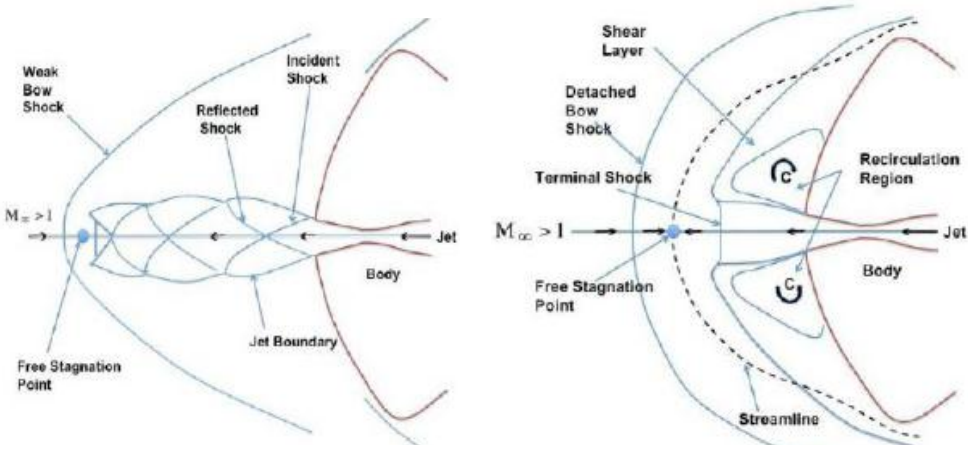

(a): Long penetration mode (b): Short penetration mode

Figure 2-3 Flow fields of long and short penetration modes [28]

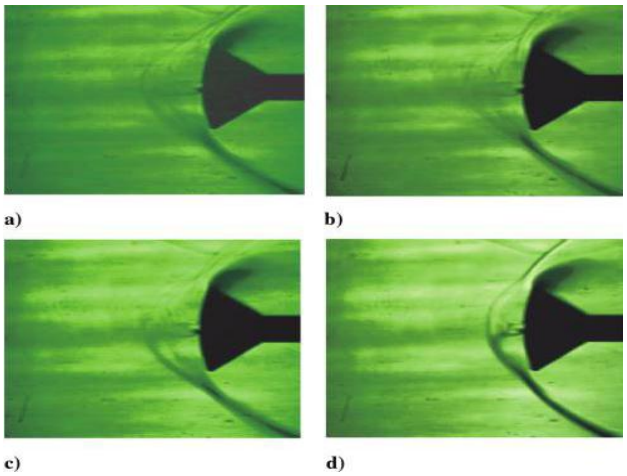

Figure 2-4 Jet Transition Mode [16]

2.2.3 Computational Research Efforts

Alongside experimental work, many efforts are also being carried out to numerically simulate the opposing jet phenomena computationally [8, 25, 29]. Hayashi [25] not only validated results with experimentations but also carried out a series of iterations varying jet exit mach number and temperatures to gain results which would have otherwise be difficult and time consuming to obtain through experiments. Through his study he showed that decrease in jet temperature decreases the heat flux (Figure 2-5). Nair *et al.* [8] validated numerical code by applying it to a number of different configurations of opposing jet. Bilal [29] numerically captured the shock standoff distance and also studied the transition mode from LPM to SPM. Figure 2-6 (a) shows shock stand-off distance from nose of body (normalized by nose radius). Figure 2-6 (b) shows transition of jet flow from LPM to SPM with increase in pressure ratio. The jet penetration depth (L) is normalized by nose radius (R).

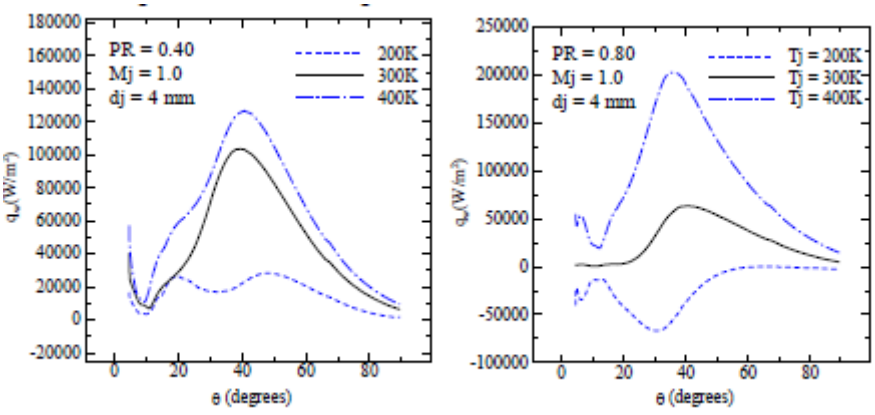

(a): PR = 0.4 (b): PR = 0.8

Figure 2-5 Variation of heat flux with jet exit temperature[25]

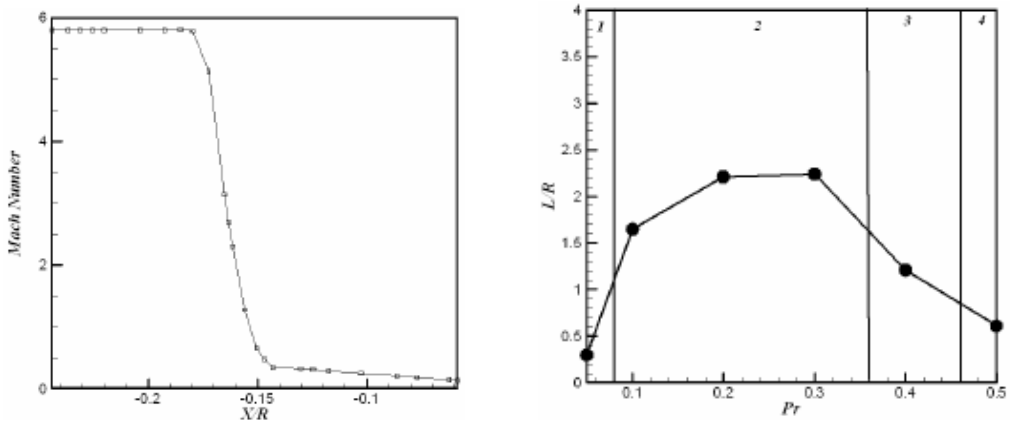

Figure 2-6 (a)Shock stand-off distance From nose of body [29] (b) Jet penetration depth vs.PR

2.2.4 Research in Different Jet Ejection Schemes

Different jet ejection schemes have also been considered. Multiple jet ejection as opposed to single jet emanating from nose of body is one of the earliest concepts considered. One of the most initial experimental works done in this regard is that of Jarvinen [30]. It is an extensive report studying different configurations, jet nozzles, mach numbers as well as effect of angle of attack. The multiple jet scheme is a very promising not only for heat reduction but also finds its application in Retro propulsion phenomenon for re-entry phase of space modules. There is however limited literature of this concept due to its difficulty in implementation experimentally, and high computational cost numerically. Cordell [31] studied numerically the works of Jarvinen [30]. Sriram [32] carried out experimental work on multiple micro jets.

One of the most recent advancements in active flow control technologies is the use of combinational strategies. In these methods, the jet is combined with other techniques such as forward cavities or aero spikes to achieve better control over flow. The works of Tamada [33] show very promising results. He showed that by the use of jet-spike combination i.e. ejection of jet from an aero spike, better drag reduction can be achieved at much lower pressure ratios. Figure 2-7 shows the use of aero spike that

reduces drag coefficient to almost half of the baseline case of Ogive body with no jet. Morimoto [34] also studied the jet-spike configuration and found a considerable reduction in heat flux.

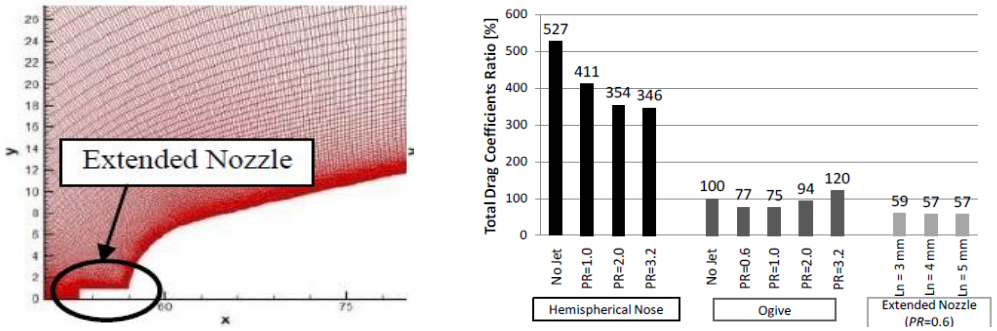

Figure 2-7 (a) Jet-Spike combination (b) Drag Coef. Of different profiles [33]

Another combination strategy is the use of forward facing jet cavity [35, 36] as shown in Figure 2-8. According to the works of Lu Haibo [35], the jet exiting the cavity meets free stream fluid which changes its direction to downstream. This forms a layer of fluid around the body protecting it from excessive heating. The present study is inspired by the jet combination strategies. It is suggested to use a divergent nozzle for jet ejection. Through a vast series of numerical simulations, an optimal nozzle configuration will be proposed that will provide better drag reduction at a lower pressure ratio.

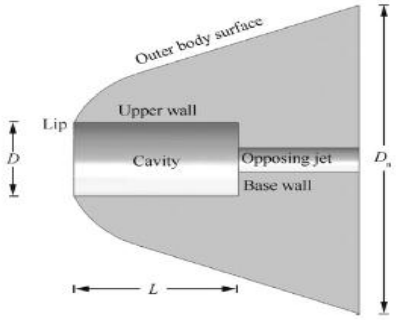

Figure 2-8 Schematic of forward facing cavity [35]

2.3 Relevant Research in Pakistan

At national level the opposing jet concept can contribute to both space exploration as well as defense applications. The race for high speed, high performance weapons of mass destruction is not a new one. In this regard Pakistan Air Force has recently inducted the Chinese CM-400AKG supersonic missile Figure 2-9 with a flight speed around Mach 4 and a hypersonic impact velocity [37]. Efforts are also underway to develop the ICBM Taimur [38]. From these endeavors it is clear that Pakistan has also entered the high speed race. Use of counter flowing jets to combat high drag profiles of high speed regimes can prove to be helpful.

Figure 2-9 CM-400AKG supersonic missile [39]

Pakistan Space and Upper Atmosphere Research Commission (SUPARCO), was established in 1961 and mandated to conduct R&D in space science. In June 1962, it became successful in launching REHBAR-I AND II becoming the third country in Asia and the tenth in the world to conduct such launching. The Space Program 2040 was initiated by Government of Pakistan in 2011. Five GEO satellites and six LEO satellites will be developed under this program. The Pico satellite ICUBE was also launched under this program in 2013 primarily aimed to contribute to space research and education. Also the Launch of Pakistan National Student Satellite Program by SUPARCO is aimed to train university students for space industry. The Sir Syed University Karachi has already joined this project [40]. Thus, the space program not only aims to tap outer space but also intends to create overall space awareness in

Pakistan through meaningful education and training programs. It is anticipated that the present work will be a good contribution to the space awareness program.

In Pakistan Zahir *et al.* [41] carried out an extensive study on the effect of mechanical spike installed on various blunt configurations in both supersonic and hypersonic regimes. Various static coefficients were computed. It was concluded that the spike helps to reduce drag but greater lengths can also affect the static stability. Among the active flow control technologies Zaidi [42] experimentally studied the effect of energy deposition on strength of shockwave in supersonic flow. The drag reduction effects achieved by an opposing jet from nose of blunt body in supersonic flow were studied by Shah and Xi-Yun Lu [29]. The numerical study was successful in not only capturing shock stand-off distances but also the transient mode of flow when jet changes from unstable region to the stable region. Bilal and Zahir [43] also carried out an interesting study on the application of cross flow jets for flight control in supersonic speeds.

From the above references it is clear that much effort is being carried out in Pakistan to study both active and passive flow control technologies to achieve greater advantages at high speeds. It is anticipated that the current research will be a beneficial contribution to these efforts.

2.4 Missing Links in Literature

Although the opposing jet phenomenon is an old concept, however it has gained importance only recently. There are many grey areas of studies that need to be brought to light. The multiple jet concept though highlighted in some researches, still needs much experimental and numerical study. Number of jets, there placement, size etc. for optimal flow behavior are all areas of study. Lack of advancement in this direction is

mainly due to the high cost required to conduct experimentations. Computational efforts in this regard are also limited because accurate simulation of multiple jet interaction with each other and simultaneously with free stream requires accurate 3-d simulations.

Other areas of study include study of transient jet ejection to gain its benefits at different stages of flight. Recent studies are looking towards combination strategies in which the jet is combined with a spike or cavity to gain more advantage. More experimental work as well combination strategies need to be suggested. The present work is inspired from the combination strategies studies. Although there is previous work on opposing jet flows through nozzles, however there is no study carrying out such a detailed analysis of nozzle geometry variations to reach optimal flow behaviors.

CHAPTER 3

NUMERICAL METHODOLOGY

3.1 Background

The main focus of the current study is to numerically calculate the drag reduction effects of opposing jet issuing from nose of a blunt body vehicle. The reason for selection of numerical procedures over experimental techniques is primarily due to the vast reduction in resources, cost and time required in conducting numerical simulations. The modeling and simulation technique used to analyze the current fluid flow problem will be Computational Fluid Dynamics (CFD).

3.2 Problem Description

The baseline configuration with available experimental data is selected from the works of Hayashi *et al.* [14]. The flow conditions are similar to those used in the experimental works of Hayashi [15] They are summarized in Table 3-1

Table 3-1 Flow Conditions

Free Stream	Gas	**Air**
	Mach No.	**3.98**
	Stagnation Pressure (MPa)	**1.37**
	Temperature (K)	**397**
Opposing Jet	Gas	**Air**
	Mach No.	**1**
	Stagnation Pressure Ratio (MPa)	**0.4, 0.6, 0.8**
	Temperature (K)	**300**
Wall	Temperature (K)	**295**

3.3 Numerical Strategy

The basic aim of the current numerical analysis is to determine the drag reduction achieved by opposing jet and its combinational strategies when ejected from nose of a hemispherical body. For this purpose, the study is divided into three phases:

- Numerical validation of no jet case
- Numerical validation of jet ejection cases at varying pressure ratios
- Numerical analysis of jet ejection from diverging nozzle

3.3.1 Numerical validation of no jet case

A numerical simulation of the simple hemispherical body without any jet was conducted. The hemispherical body was 50 mm in diameter as shown in Figure 3-1. Grid independence study was also carried out. The surface pressure data were duly validated with experimental results.

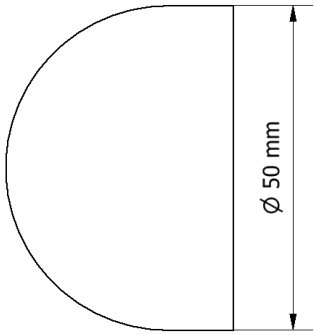

Figure 3-1 Simple Hemispherical Body without Jet

3.3.2 Numerical validation of jet ejection cases at varying pressure ratios

In the present work, the jet ejection diameter is kept constant at 4 mm as shown in Figure 3-2. The free stream conditions are also kept constant. However the Pressure

Ratio (PR) is varied. PR is defined as ‘the ratio of jet total pressure to free stream total pressure.

$$P.R. = \frac{P_{oj}}{P_{o\infty}}$$

Flow analysis was conducted at three different pressure ratios i.e. P.R = 0.4, 0.6 and 0.8. Surface pressure data was duly validated with corresponding experimental results.

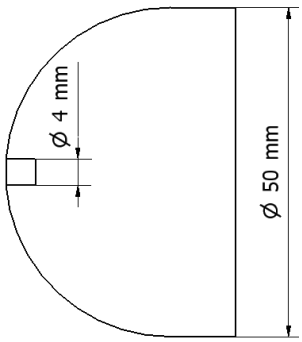

Figure 3-2 Hemispherical Body with Jet

3.3.3 Numerical analysis of jet ejection from divergent nozzle

Once the basic grid and computational strategy was finalized, an effort was made to reduce surface pressure values on the blunt body through geometric variations of jet ejection schemes.

Recent efforts have shown that jet ejected from a cavity can provide better results than jet ejected directly from nose of the body. In this regard the effect of jet ejected from a divergent nozzle was studied. The effect of nozzle geometric variations i.e. angle of and length of nozzle were also computed. The nozzle was tested at three angles θ= 5 °, 10 ° and 15 °. At each angle the nozzle length was varied to 4, 8, 12 and

16 mm. Each geometric case was tested at all three pressure ratios i.e. 0.4, 0.6 and 0.8. This created a three dimensional matrix of dimensions 4*3*3 summing to a total of 36 simulations. Thus an extensive numerical analysis was conducted to reach an optimal configuration under the given parameters that would impart minimum drag to the blunt profile under study. Figure 3-3 is a pictorial summary of the various geometric iterations studied.

Table 3-2 lists details of all the cases simulated. Each case is assigned a particular notation for example L4 (5). The number following L denotes the length of nozzle and the number in brackets corresponds to nozzle divergent angle. So L4 (5) means a nozzle of length 4 mm and divergent angle of 5°.

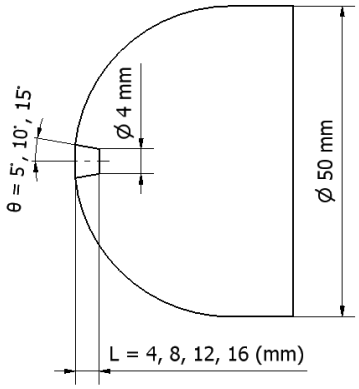

Figure 3-3 Hemispherical Body with Jet Ejected from Divergent Nozzle

Table 3-2 Summary of Cases Run

Sr no	P.R	Case	Nozzle Length (mm)	Nozzle Divergent Angle (deg °)
1.	0	No jet	-	-
2.	0.4	Jet 0.4	-	-
3.	0.6	Jet 0.6	-	-
4.	0.8	Jet 0.8	-	-
5.	0.4	L4 (5)	4	5
6.		L8(5)	8	5

7.		L12(5)	12	5
8.		L16(5)	16	5
9.		L4 (10)	4	10
10.		L8(10)	8	10
11.		L12(10)	12	10
12.		L16(10)	16	10
13.		L4 (15)	4	15
14.		L8(15)	8	15
15.		L12(15)	12	15
16.		L16(15)	16	15
17.	0.6	L4 (5)	4	5
18.		L8(5)	8	5
19.		L12(5)	12	5
20.		L16(5)	16	5
21.		L4 (10)	4	10
22.		L8(10)	8	10
23.		L12(10)	12	10
24.		L16(10)	16	10
25.		L4 (15)	4	15
26.		L8(15)	8	15
27.		L12(15)	12	15
28.		L16(15)	16	15
29.	0.8	L4 (5)	4	5
30.		L8(5)	8	5
31.		L12(5)	12	5
32.		L16(5)	16	5
33.		L4 (10)	4	10
34.		L8(10)	8	10
35.		L12(10)	12	10
36.		L16(10)	16	10
37.		L4 (15)	4	15
38.		L8(15)	8	15
39.		L12(15)	12	15
40.		L16(15)	16	15

3.4 Numerical Model

Precise simulations depend entirely upon the accuracy of formulation of numerical model. Details of numerical modeling and solver settings are provided in the sections to follow.

3.4.1 Computational Grid and Boundary Conditions

A fully structured 2D axis symmetric computational grid was generated in the commercial software Gambit®. Due to symmetry of the problem only half of the geometry was modeled. The grid is highly clustered near the body surface and jet orifice in order to accurately resolve complex flow features in these regions. The jet flow boundary was set to pressure inlet. The numerical domain was modeled as Farfield with outlet modeled as pressure outlet. The selection of these boundary conditions successfully allowed to compute overall mass flow rate of the system and check its conservation. A no slip isothermal condition was applied to the wall. The numerical grid along with the prescribed boundary conditions is shown in Figure 3-4

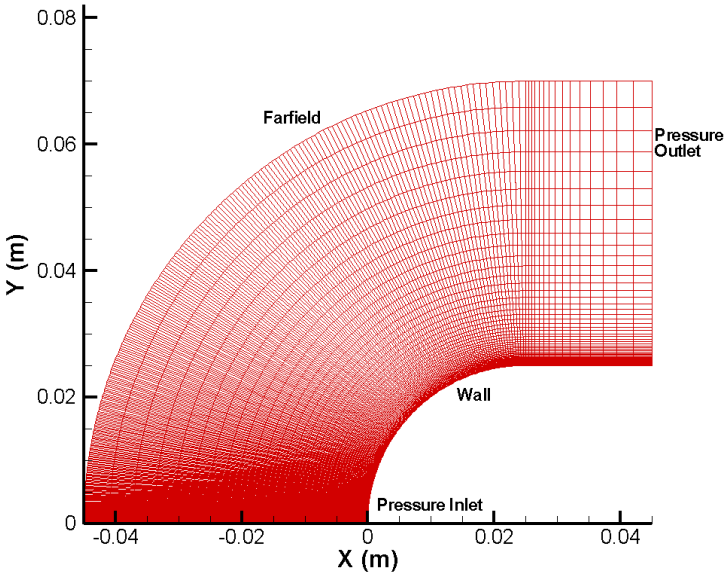

Figure 3-4 Numerical Grid with Boundary Conditions

3.4.2 Solver Conditions

The commercially available software ANSYS® FLUENT was used as the numerical solver for all the simulations. Axis symmetric Steady state Reynolds-Averaged Navier-Stokes (RANS) equations were solved using density based implicit solver. Density based formulations solve the governing equations (mass, momentum and energy) simultaneously. Density is the primary variable deduced from mass or continuity equation and pressure is then determined using equation of state. This solver is found to work efficiently in supersonic flows.

The air is modeled as ideal gas as aerothermochemical considerations can be neglected for the current operating conditions. Air viscosity is defined by Sutherland's viscosity law. In order to accurately capture complex flow features such as shockwaves, separation and recirculation regions; a turbulence model was introduced. The K-ω SST turbulence model with default values was used. This model uses a blending function which activates the K- ω model to accurately capture near wall effects and converts to the more efficient K-ε formulations for the free stream conditions.

CHAPTER 4

Results and Discussion

4.1 Background

A vast series of simulations are conducted. Mach contour as well as surface pressure plots are validated with available experimental results for both no jet and jet ejection cases from hemisphere body. Finally results are presented by introducing a diverging nozzle at nose of hemispherical body and varying both length and angle of the nozzle to determine effect on surface pressure and drag experienced by hemisphere body.

4.2 Baseline Computations

In order to validate the numerical procedure, initial computations were carried out on the baseline cases. Experimental data was available for the simple hemispherical body in supersonic flow without counter flowing jet. Similarly surface pressure plots were also available for the jet injection cases ranging from P.R=0.4, 0.6, 0.8. Numerical simulations for the four baseline cases were conducted and surface pressure plots were duly validated with experimental data. A detailed discussion of the baseline results is presented.

4.2.1 Baseline Computation (No Jet Case)

The most eminent feature of a blunt body in supersonic flow is formation of a bow shock wave. Other features include a boundary layer and shock layer. The bow shock is very thin and clearly visible just head of the blunt body. The boundary layer is

the region closest to the body with thickness slightly greater than bow shock. The shock layer includes the boundary layer and extends all the way to the bow shock wave. The computed density contours are shown in Figure 4-1. The density contours show that the computed shock stand-off distance is in well agreement with experimental images obtained from the works of Hayashi[15].

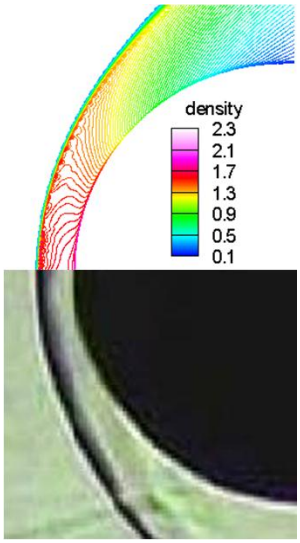

Figure 4-1 Comparison of Density Contours (kg/m3) with Experimental Images

A grid independence study was also conducted for the no jet case as shown in Figure 4-2. Three grids; coarse (45000) medium (67000) and refine (116000) were used. The results of the medium grid matched very closely with the fine grid as well as with the experimental surface pressure plots. The medium grid was selected for further analysis.

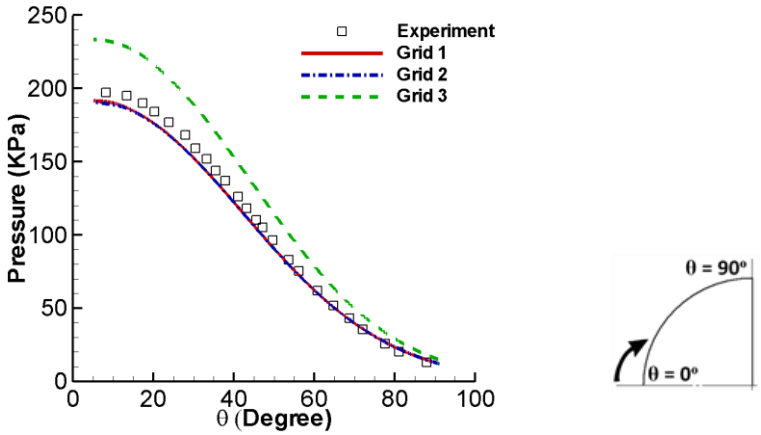

Figure 4-2 Grid Independence Study of no Jet Case

4.2.2 Baseline Computation (Jet Injection Cases)

The jet issuing from the nose of blunt body is specified in terms of total pressure ratio P.R. It is the ratio of jet stagnation pressure P_{oj} to free stream stagnation pressure $P_{o\infty}$. Three different pressure ratios were tested during experiments i.e. P.R. 0.4, 0.6 and 0.8. Numerical simulations of all three pressure ratios were conducted and duly validated with experimental surface pressure data. Figure 4-3 shows both numerical and experimental surface pressure plot at three pressure ratios. The computed results are found to be in good agreement with the findings of Hayashi [15]. The plot also indicates a decrease in surface pressure with increase in pressure ratio.

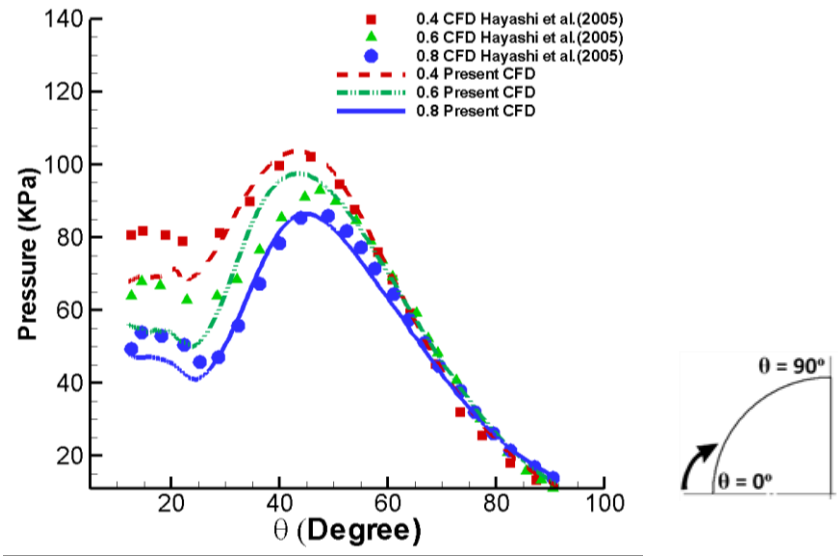

Figure 4-3 Surface Pressure Distributions at Various Pressure Ratios

Figure 4-4 and Figure 4-5 show computed Mach number contours and density contours compared with experimental images at three pressure ratios respectively. The results indicate that the numerical analysis is successful in capturing all features of jet interaction.

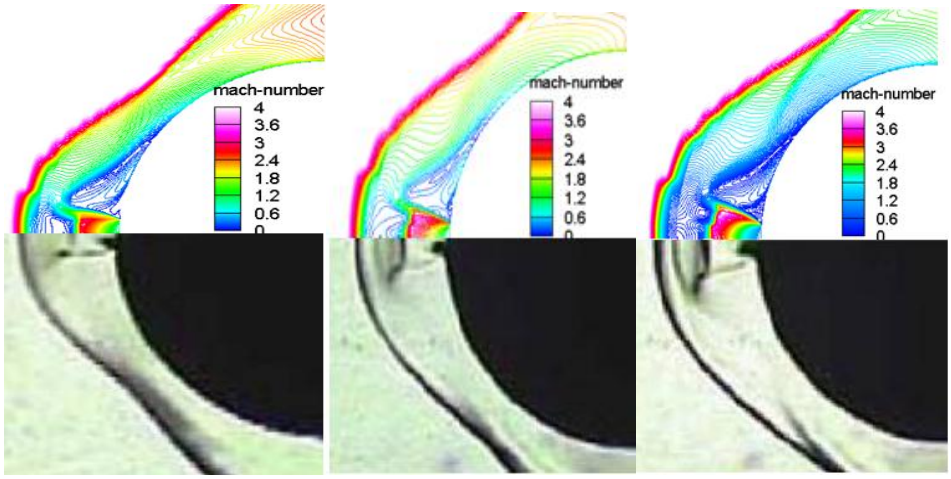

Figure 4-4 Comparison of Mach Contours with Experimental Images [15] for Jet Cases

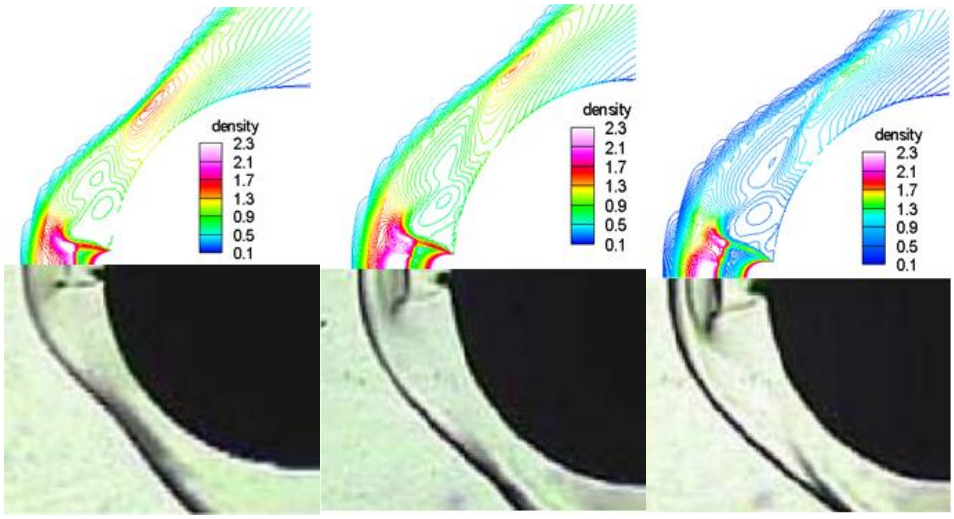

Figure 4-5 Comparison of Density Contours (kg/m^3) with Experimental Images for Jet Cases

4.3 Effect of Divergent Nozzle

The basic aim of the current endeavor is to determine a method to minimize the drag experienced by a blunt body in high speed flow. For this purpose a divergent nozzle was introduced in the fore body region of the blunt body to determine its effect on flow field structures. A series of geometric iterations were conducted by varying both the length and angle of the divergent nozzle at all three pressure ratios. The iterative procedure was adopted in order to suggest an optimal pressure ratio + nozzle geometry combination under the given conditions.

During the numerical analysis both LPM and SPM modes as well as flow separation was observed. General trends were also noticed with length and angular variation of nozzle. A detailed discussion of these trends along with possible reasoning is presented in this section.

4.3.1 General Flow Field Structures

An initial assessment of the CFD result can be made by comparison of flow field structures of nozzle jet ejection cases with those mentioned in theory.

4.3.1.1 Operating Conditions of Jet Flows

Jet flows through nozzles generally have three different configurations depending upon operating conditions which are dictated by the ambient static pressure (P_∞) as well as nozzle exit static pressure (P_e). If nozzle exit pressure is less than ambient pressure then flow is said to be Over-Expanded. The jet collapses towards the central axis through a series of shock waves in order to increase the pressure to ambient pressure at nozzle exit (Figure 4-6). Flow separation and subsequent formation of shockwaves inside the nozzle is a highly turbulent and is considered an undesirable phenomenon.

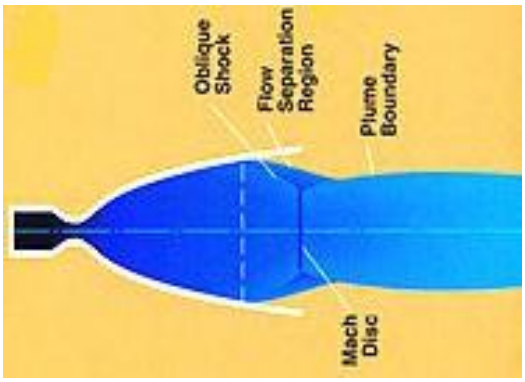

Figure 4-6 Flow Conditions for Over Expanded Nozzle [44]

If the nozzle exit pressure is slightly greater than ambient pressure the nozzle is said to be under-expanded. The jet forms a plume structure at nozzle exit, however the expansion waves reflected from the jet boundary form compression waves. A series of compression and expansion waves form a diamond shaped pattern in the flow until ambient pressure is reached Figure 4-7.

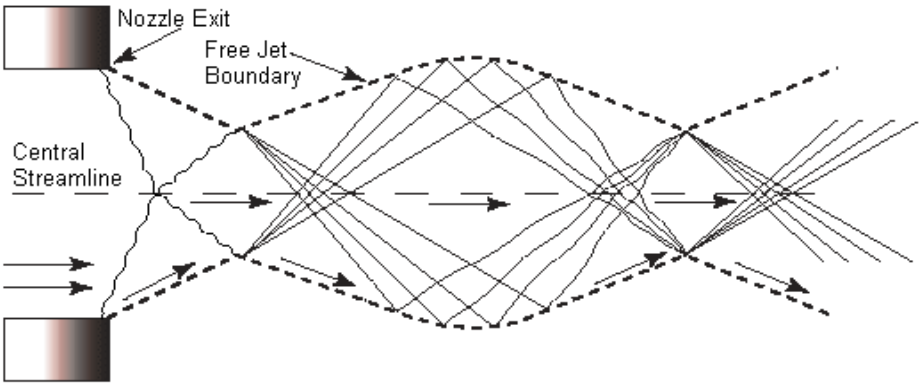

Figure 4-7 Flow Conditions for Under Expanded Nozzle[45]

If the nozzle exit pressure is much greater than free stream ambient pressure (4 to 5 times greater) then the nozzle is said to be highly under expanded. The jet plume structure is terminated by a strong normal shockwave called as Mach Disc. Figure 4-8 shows some of the distinct flow features which can be observed in this mode.

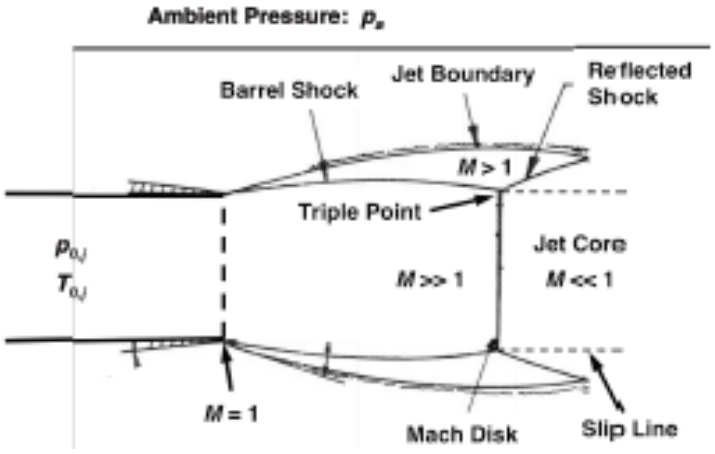

Figure 4-8 Flow Conditions for Highly Under Expanded Nozzle [31]

The jet exiting from nozzle undergoes expansion until the jet pressure equals the ambient pressure, thus forming a constant pressure jet boundary. Jet is reflected from jet boundary in the form of weak compression waves collectively forming a barrel shock. The rapid expansion in the jet core reduces the axial pressure to a limiting value at which a strong normal shock wave occurs. This is referred to as a mach disc or terminating shock. Flow upstream of the normal shock is highly supersonic whereas

downstream flow is sub sonic. Flow beyond the barrel (oblique) shock is also supersonic but at lesser value then supersonic jet core. At the intersection point of barrel shock and mach disc a reflected shock emanates due to which this region is called as triple point. Jet flow passing through the reflected shock remains supersonic whereas flow passing through mach disc becomes subsonic. A slip line is defined in flow separating the external supersonic flow from inner subsonic jet core.

4.3.1.2 Interaction of Free Stream with Opposing Jet Flows

The introduction of an opposing jet in supersonic free stream flows can give rise to two distinct flow modes. These flow regimes or modes have been identified in literature as the unstable Long Penetration Mode (LPM) and the stable Short Penetration Mode (SPM). The occurrence of these modes is a strong function of jet to free stream pressure ratios.

The over expanded jet is at a lower pressure than free stream pressure. This may cause shock waves and subsequent flow separation inside the nozzle. This is a highly turbulent and undesired phenomenon.

The under expanded jet is at a slightly greater pressure (1-2 times greater) than free stream. A series of compression and expansion waves form a diamond shaped pattern in the flow until ambient pressure is reached. This diamond shaped pattern can rupture the bow shock wave ahead of the blunt body in supersonic flow. This causes the occurrence of the long penetration mode. Figure 4-9 shows both schematic and experimental images of LPM mode as well as an image of LPM mode captured from current numerical analysis. This is also an undesirable unstable mode in which the shockwave is either diffused or oscillates axially. This mode is difficult to simulate

numerically as it requires unsteady transient 3-d simulations to fully capture shock oscillations and there subsequent pitching effect imparted on blunt body.

(a) (b) (c)

Figure 4-9 Flow conditions for LPM (a) Schematic [28] (b) Experimental [16] (c) Computational

The highly under expanded jet is at a much greater pressure (greater than three times) than free stream. A highly under expanded jet interacting with opposing free stream flow is desirable as it leads to the formation of the stable short penetration mode. Free stream supersonic flow ahead of blunt body is decelerated to subsonic by the bow shock wave. The supersonic jet flow is decelerated to subsonic by the mach disc. The two subsonic flows interact at the stagnation point. A contact surface arises from the stagnation point separating the subsonic free stream and jet flows. The interaction of free stream and jet flow produces a recirculation region over the body. This recirculation region emanates at the intersection point of terminating and barrel shock and stagnates on coming in contact with body. This recirculation region moves radially outwards with the increase in jet pressure. At a certain jet pressure the recirculation region completely clears the fore body and reattaches downstream forming a layer of protective fluid in the fore body vicinity, protecting it from high pressure and temperature loads.

The mode of penetration with distinct flow features described in literature above is called the *blunt penetration mode*. This is a desirable mode in which the flow remains stable and the shock wave is not bifurcated. The jet increases shock stand-off distance and its recirculation forms a protective layer over the body. This phenomenon has been found to significantly reduce fore body heat and drag loads. Figure 4-10 shows both schematic and experimental images of SPM mode as well as an image of SPM mode captured from current numerical analysis.

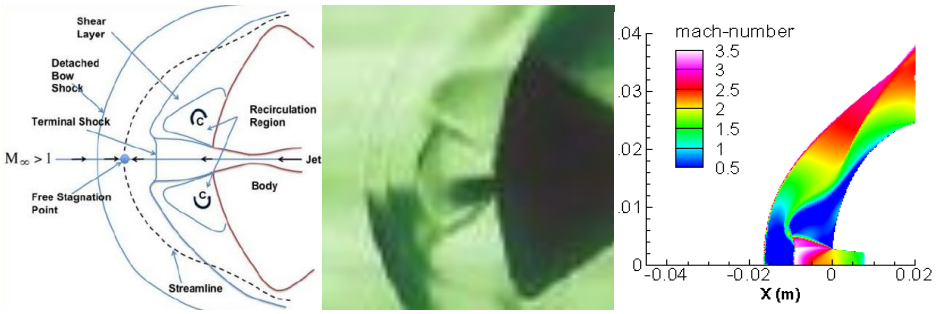

(a) (b) (c)

Figure 4-10 Flow conditions for SPM (a) Schematic [28] (b) Experimental [16] (c) Computational

4.4 Effect of Divergent Nozzle and its Geometric Variations:

In the present study both SPM and LPM modes as well as flow separation was observed during various simulations. The theory above presents a good reasoning for the occurrence of these phenomena. The results to follow discuss the various cases simulated and flow modes found for each simulation. The axial Mach number and pressure plots are used to determine the LPM or SPM flow conditions. The mach contour images are used for flow visualization to display LPM, SPM or flow separation. The surface pressure plots are used to compare the pressure acting on the surface of body under different conditions. The cases exhibiting flow separation are omitted from axial mach and pressure plots as flow separation has -three dimensional effects which are not captured accurately by the current two dimensional simulations.

Similarly, cases exhibiting LPM are omitted from surface pressure plots as the present steady state simulations cannot capture the transient effects of LPM mode.

For clarity, it is once again recapped that all the simulations are assigned a particular notation for example L4 (5). The number following L denotes the length of nozzle and the number in brackets corresponds to nozzle divergent angle. So L4 (5) means a nozzle of length 4 mm and divergent angle of 5 °.

4.4.1 Effect of Geometric Variations at P.R = 0.4

The computed baseline case of simple jet ejected from nose of body showed SPM. This result was also found in experiments as can be seen from Figure 4-4. However Hayashi [15] in his findings stated that P.R. = 0.4 was the lower limit at which flow just enters the SPM mode. A well-defined SPM mode was more clearly visible in P.R. = 0.6, 0.8 cases. In the current analysis, only the smallest nozzle case L4 (5) showed SPM, whereas all other length and angular variations showed LPM mode or flow separation inside nozzle for the P.R. of 0.4 cases. The PR of 0.4 cases therefore did not exhibit any favorable results.

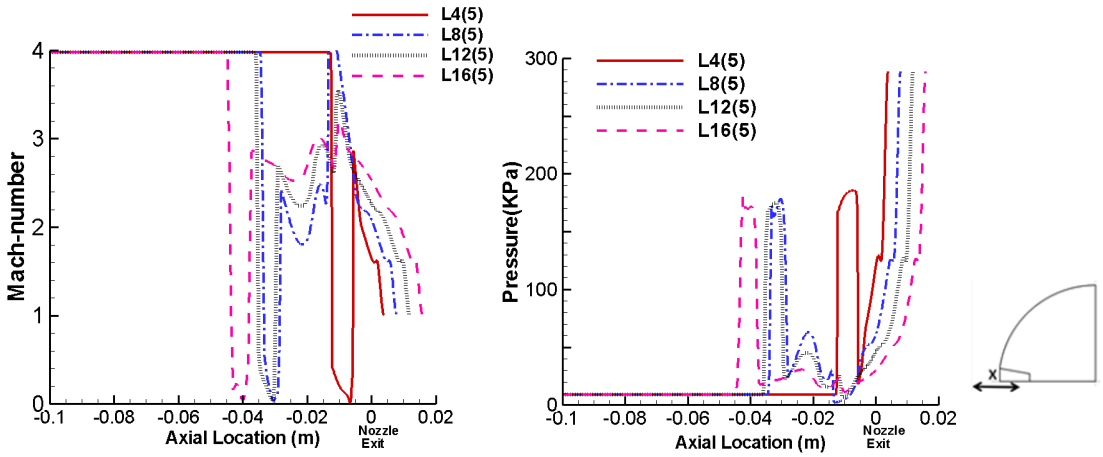

Figure 4-11 Mach number and pressure distributions along jet axis at different lengths for P.R. = 0.4, θ = 5 °

Figure 4-11 shows axial pressure and Mach number variation respectively at different lengths for θ = 5 °. Only the first case L4 (5) shows SPM mode, all other cases show LPM. The axial Mach and pressure plots assist in determining whether flow is SPM or LPM. As shown in Figure 4-12 if the axial plot exhibits two distinct shock waves (labeled bow shock and terminal shock in Figure 4-12) without a series of weak compression and expansion waves, then it is said to be in SPM. If however the flow displays a series of compression and expansion waves together with a long shock stand-off distance, then it is said to be in LPM.

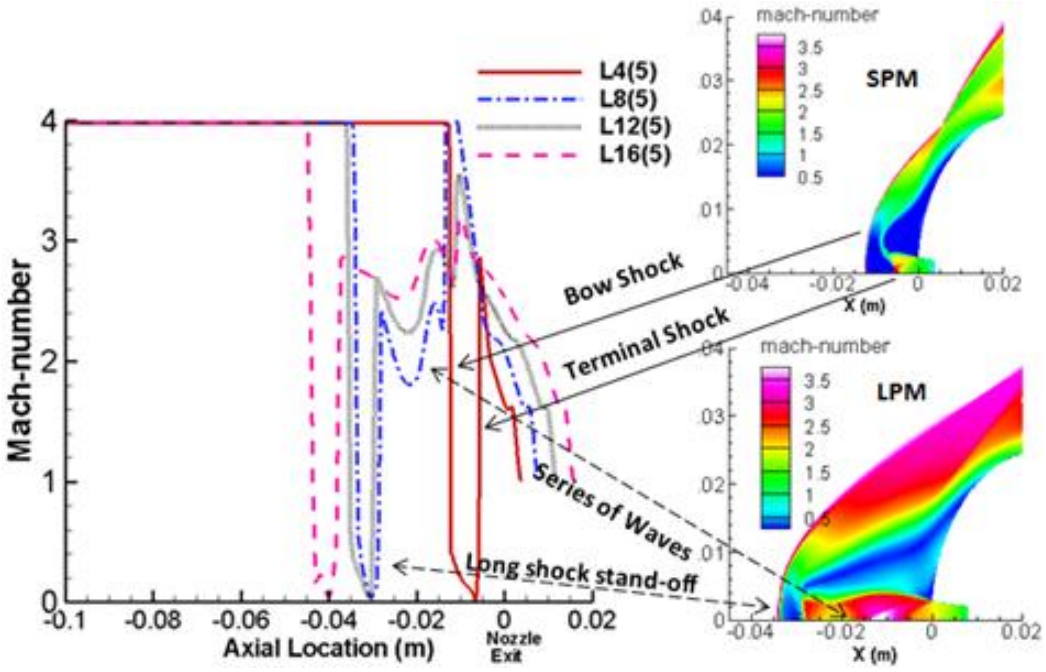

Figure 4-12 Identification of Different Flow Modes from Computed Results

Figure 4-13 show Mach contour plots at PR = 0.4 for θ = 5 °and 10 ° cases. Figure 4-13 (a) shows that at P.R. = 0.4 for a small divergent angle θ = 5 °, only the first case L4 (5) shows SPM mode, all other cases show LPM. Figure 4-13 (b) shows mach contour plots at PR = 0.4 for θ = 10 °. The first case L4 (10) shows LPM mode, whereas all other cases show flow separation with in nozzle. The separation becomes

more pronounced with increase in nozzle length. Results of θ = 15 ° cases are not presented as they exhibit a similar flow separation scenario.

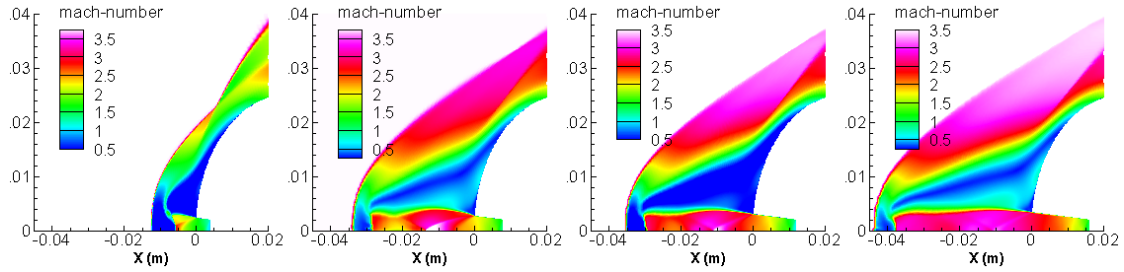

(a) θ = 5 °

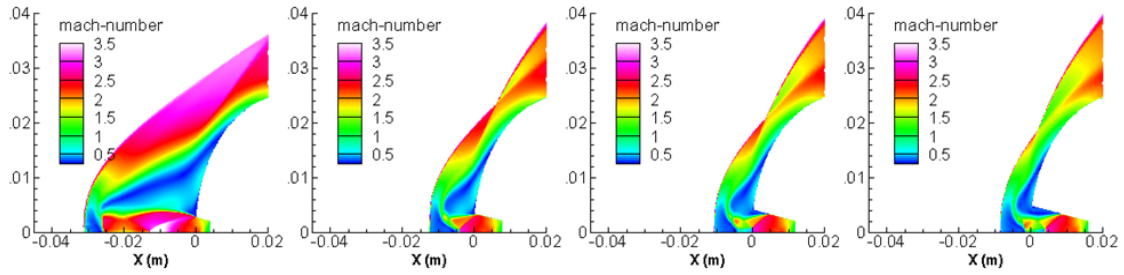

(b) θ = 10 °

Figure 4-13 (a-b) Variation of Mach contour plots at PR = 0.4 with variation in Nozzle Lengths (4, 8, 12, 16 mm) and Angles (θ = 5 ° and 10 °).

The flow separation phenomenon occurs within nozzle due to flow of fluid in reverse direction. For a supersonic divergent nozzle, the static pressure continuously decreases with increasing area. At PR= 0.4, the static pressure of the jet is low. Flow along the nozzle causes further reductions of pressure to such low values that flow separations occurs and reverse flow is observed. This is a highly unstable and undesirable phenomenon [46]which generates strong side forces. Flow features no longer remain symmetric and three dimensional effects must be considered. In the current analysis only contour plots of flow separation are included and corresponding axial pressure or Mach number plots are not presented as they do not include three dimensional effects.

4.4.2 Effect of Geometric Variation at P.R = 0.6

For a small nozzle divergent angle, θ = 5 °, increase in nozzle length up to 12 mm showed favorable reduction in surface pressure. However the case L16 (5) at P.R. = 0.6 showed LPM mode. The SPM mode for first three lengths and shift to LPM mode for L16 (5) case can be seen from axial mach and pressure plots of Figure 4-14.

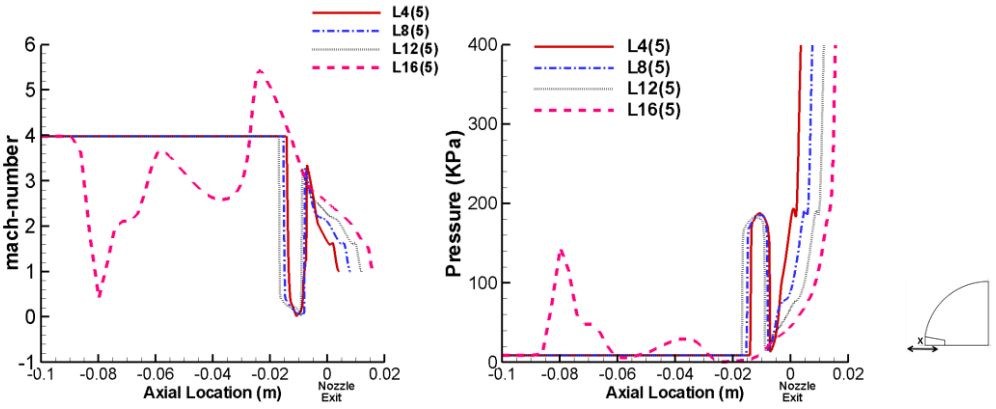

Figure 4-14 Mach number and pressure distributions along jet axis at different lengths for P.R. = 0.6, θ = 5 °

Figure 4-15 shows mach contours for the effect of length variation at P.R. = 0.6, for θ = 5 °, 10 °and 15 ° cases. It can be seen from Figure 4-15 (a) that at θ = 5 °, flow remains in SPM for the first 3 lengths and then shifts to the LPM for L 16 (5) case. The shift from SPM to LPM is possibly due to the change in jet flow conditions from highly under-expanded to the under expanded jet as mentioned in the literature above. Also the size of recirculation region and bluntness of bow shockwave increases for the first 3 lengths. A greater size of the recirculation region means the flow reattaches further down the fore body region, hence providing a better shielding effect to the blunt body and reducing the surface pressure. Similar results can be deduced from the surface pressure plots of P.R. = 0.6, θ = 5 ° case in Figure 4-16 (a). Thus for the P.R. = 0.6, θ = 5 ° case increase in length is advantageous up to L=12mm after which flow becomes unstable.

Figure 4-15 (b) shows mach contours for the effect of length variation at P.R. = 0.6, θ = 10 °. The flow remains in SPM for the first 3 lengths after which it exhibits flow separation. The recirculation region remains almost the same for the first two lengths after which it reduces for L 12 (10) case. This behavior can also be observed from the surface pressure plots of Figure 4-16 (b). This means that at higher nozzle divergent angle (θ = 10 °) increase in length is advantageous only up to L=8 mm after which it becomes disadvantageous. The last case i.e. L= 16 mm shows flow separation because pressure reduces to such an extent along the divergent nozzle that it causes the jet to become over expanded. Hence flow separation and subsequent shockwaves occur inside the nozzle to reach ambient pressure conditions. A similar trend can be observed for the P.R. = 0.6, θ = 15 ° cases in Figure 4-15 (c). Only the first two lengths are in SPM after which flow separation occurs. There is a marked shrinkage in the recirculation region for the L= 8 mm case. This means only the first case i.e. L4 (15) gives the best results after there is no further advantage in increasing length. . Similar results can be deduced from the surface pressure plots of Figure 4-16 (c)

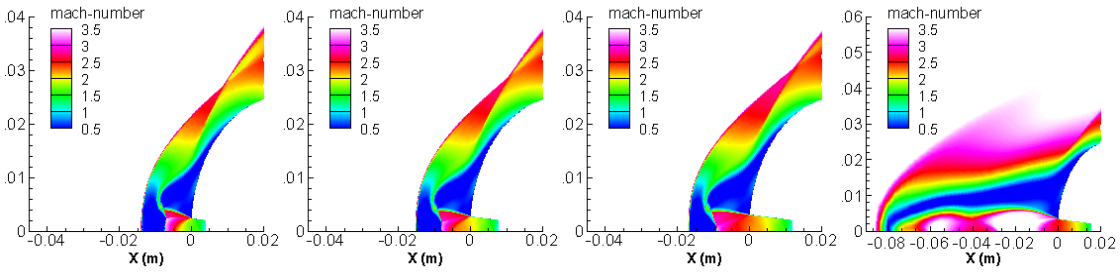

(a) θ = 5 °

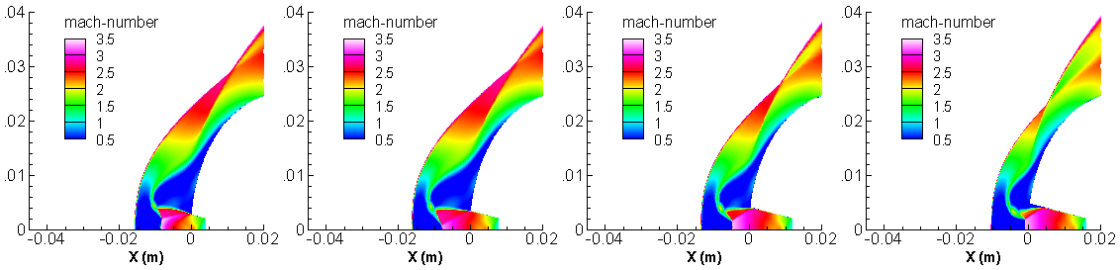

(b) θ = 10 °

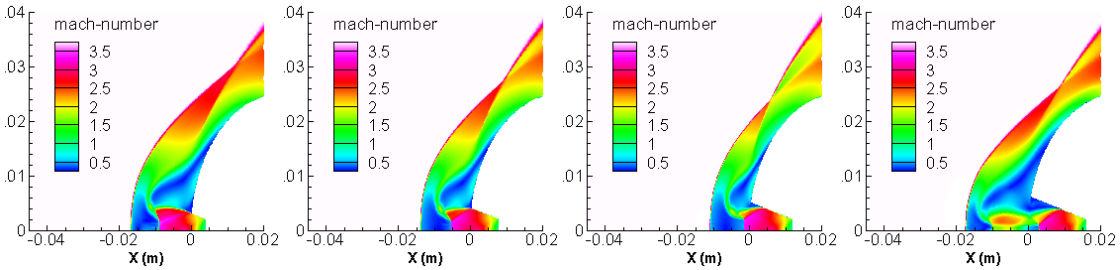

(c) θ = 15 °

Figure 4-15 (a-c) Variation of Mach contour plots at PR = 0.6 with variation in Nozzle Lengths (4, 8, 12, 16 mm) and Angles (θ = 5 ° ,10 ° and 15°)

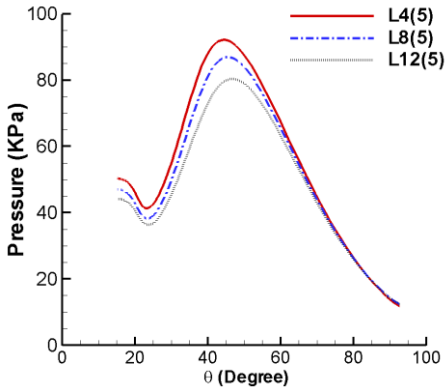

(a) θ = 5 °

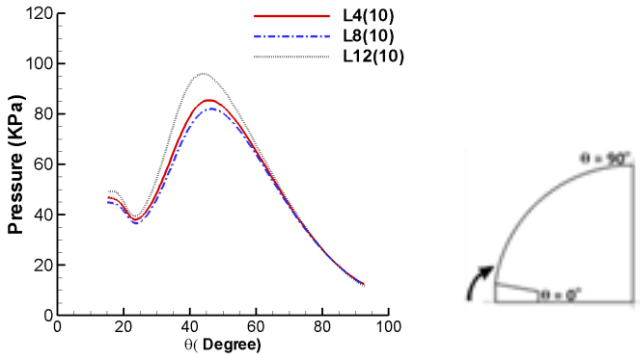

(b) θ = 10 °

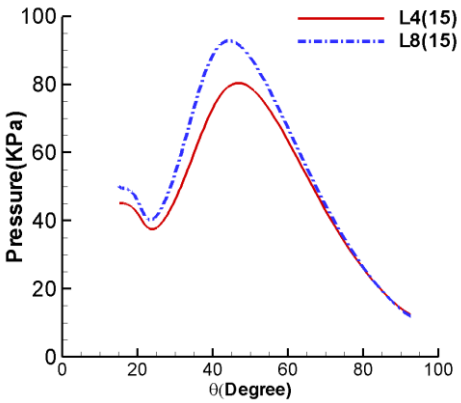

(c) θ = 15 °

Figure 4-16 Variation in Surface Pressure Distributions with Nozzle Length at PR = 0.6 for θ = 5 °, 10 ° and 15 ° cases.

Figure 4-16 (a - c) shows surface pressure variations with change in nozzle length at P.R. = 0.6 for the three divergent angles θ= 5 °, 10 °, 15 °. Cases exhibiting LPM or flow separation have been omitted from the plots as both these features have 3d effects which cannot be captured by the current 2d simulations. From the graphs it can be seen that the cases L12 (5) and L4 (15) give the lowest values of surface pressures.

The Length and angle variations at P.R = 0.6 show that at smaller values of divergent angle; nozzle of greater length is advantageous. However, the reverse is true for higher values of divergent angle, where nozzle of smallest length gives the lowest surface pressure values. To summarize, at P, R = 0.6 three cases L12 (5), L8 (10), and L4 (15) gave the smallest value of surface pressure. Any of these three cases can be selected as the optimal nozzle configuration at P.R = 0.6 based on its advantage in physical implementation.

4.4.3 Effect of Geometric Variation at P.R = 0.8

For small divergent angle θ = 5°, flow remains in SPM mode for all lengths at P.R. = 0.8, Figure 4-17.

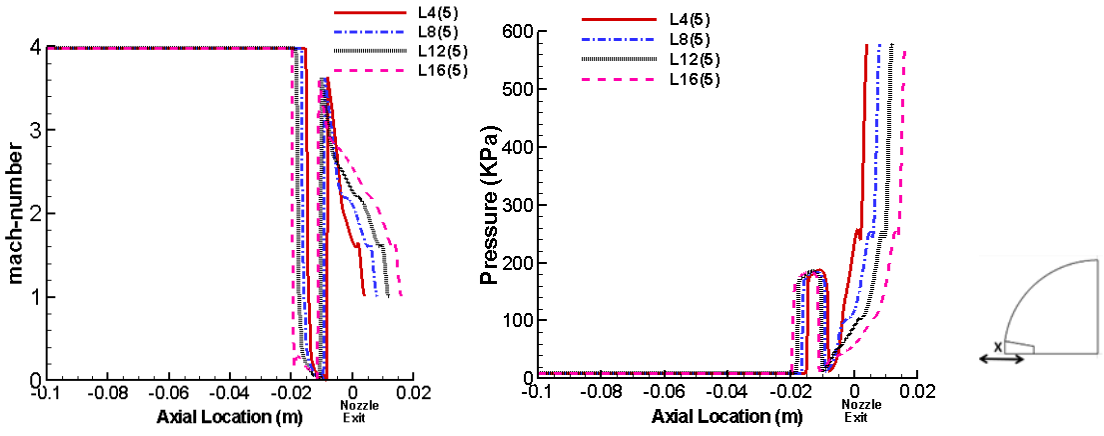

Figure 4-17 Mach number and pressure distributions along jet axis at different lengths for P.R. = 0.8, θ = 5 °

For P.R. = 0.8 θ = 5 ° cases, the well-defined SPM flow can be seen from the mach contour images of Figure 4-18 (a). The recirculation region as well as shock stand-off distance increasing with increase in length from L = 4 to L = 16 mm. The case L16 (5) giving lowest value of surface pressure as can be seen from surface pressure plots of Figure 4-19 (a). This behavior is similar to that expected from theory. The high P.R of jet causes it to be highly under-expanded at nozzle exit, keeping flow in the stable SPM mode even for the greatest length of 16 mm cases. The greater length of the nozzle at low divergent angles seems to be more advantageous, allowing the flow to fully develop at nozzle exit. Similar to the previous findings, the smallest nozzle divergent angle, θ = 5° gives the best results at largest length L=16 mm.

For θ = 10 °, flow remains in SPM at all lengths Figure 4-18 (b). However, the shock stand-off distance and recirculation region slightly reduce for the L12 (5) case. The reduction becomes more pronounced with increase in length i.e. L 16 (5) case. A similar trend can be noticed in the surface pressure plots of Figure 4-19 where there exists a point of inflexion from L8 (10) to L12 (10) case. The surface pressure decreases up to L8 (10) after which it once again begins to increase with increase in length for the L12 (10) and L16 (10) cases. This means that at higher nozzle divergent angle (θ = 10 °) increase in length is advantageous only up to L=8 mm after which it becomes disadvantageous. Similarly for θ = 15 ° cases only L4 (15) case gives the lowest value of surface pressure. Further increase in length causes an increase in surface pressure until flow separation occurs for the maximum length L = 16 mm case

as can be seen from Figure 4-18 (c) and Figure 4-19 (c). Hence at large divergent angle θ = 15° the smallest length case L 4(15) gives the most advantageous results.

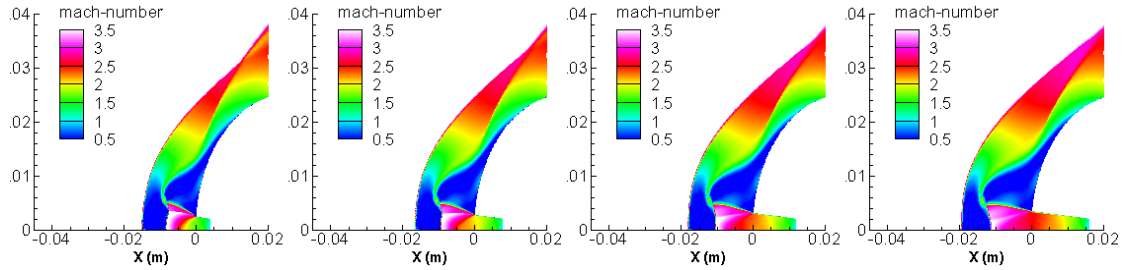

(a) θ = 5 °

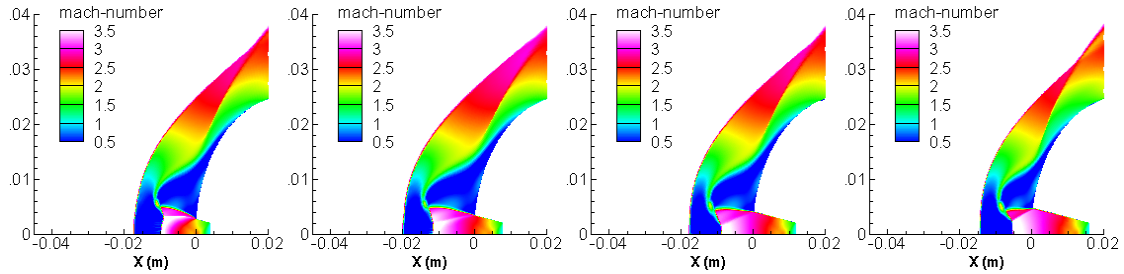

(b) θ = 10 °

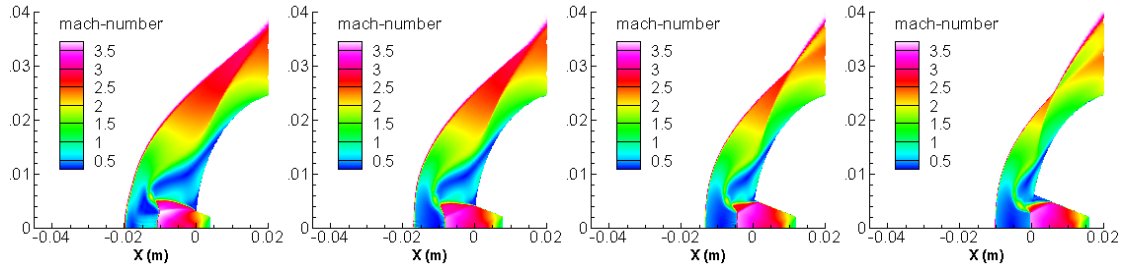

(c) θ = 15 °

Figure 4-18 (a-c) Variation of Mach contour plots at PR = 0.8 with variation in Nozzle Lengths (4, 8, 12, 16 mm) and Angles (θ = 5 ° ,10 ° and 15°).

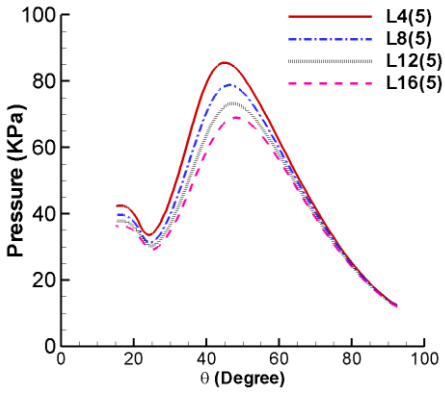

(a) θ = 5 °

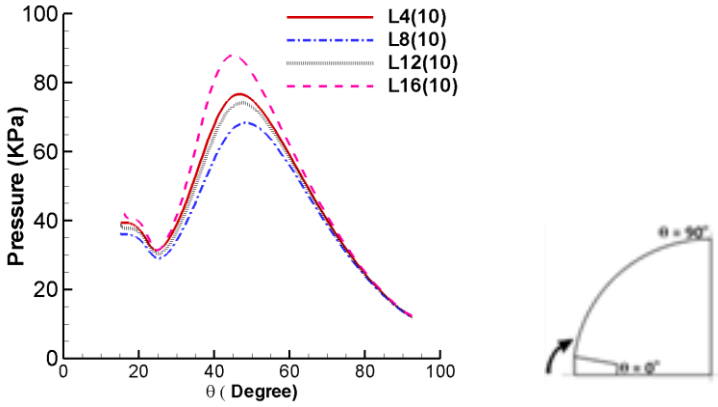

(b) θ = 10 °

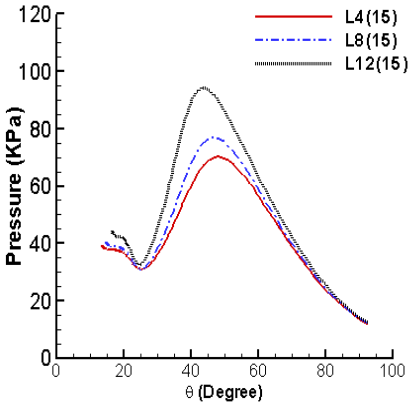

(c) θ = 15 °

Figure 4-19 Variation in Surface Pressure Distributions with Nozzle Length at PR = 0.8 for θ = 5 °, 10 ° and 15 ° cases.

Figure 4-19 (a-c) shows surface pressure variations with change in nozzle length at P.R. = 0.8 for the three divergent angles θ= 5 °, 10 °, 15 °. The linear trend of better surface pressure results with increase in length can be seen in Figure 4-19 (a), this trend continues to Figure 4-19 (b), however the reverse phenomena begins to occur at greater lengths of Figure 4-19 (b) where surface pressure increases with increase in length. This reverse trend follows through to the greater divergent angle θ = 15 ° cases of Figure 4-19 (c). From Figure 4-19 (a-c) it can be deduced that the cases L 16 (5), L 8 (10) and L4 (15) give the lowest surface pressure values. Any of these three cases can be selected as the optimal nozzle configuration at P.R = 0.8 based on its advantage in physical implementation.

4.5 Effect of Geometric Variations on Drag Coefficient

The main purpose of the current endeavor was to assess the amount of drag reduction achieved by inserting a divergent nozzle at the nose of a blunt hemispherical body. The surface pressure results of the previous discussion show that a considerable reduction in drag is achieved. In order to compare the drag reduction achieved in each case and gain a better understanding of the effect of various geometric variations, results are summarized in the form of a bar chart in Figure 4-20. The figure shows the percentage reduction in drag coefficient for each case. The selected baseline case was the simple hemispherical blunt body without any jet. Since the P.R. = 0.4 divergent nozzle cases did not produce any fruitful results hence they are omitted from Figure 4-20. All cases exhibiting LPM or flow separation have not been included and only cases displaying the stable SPM flow have been summarized.

From Figure 4-20 it can be seen that a maximum of approximately 40 % drag reduction can be achieved at P.R = 0.8 without the use of any nozzle. By the use of a

divergent nozzle the same reduction can be achieved at a lower pressure ratio 0.6. A maximum of 46 % [L 4 (15) case] drag reduction can be achieved at P.R = 0.6 with nozzle. Shifting to the P.R = 0.8 nozzle cases a maximum of 56 % drag reduction can be achieved [L8 (10) case]. For each pressure ratio, a general trend can be noticed. At lower divergent angles, the greater length provides a greater drag reduction. However at higher divergent angles, the reverse phenomena occurs a greater lengths cause a decline in drag reduction.

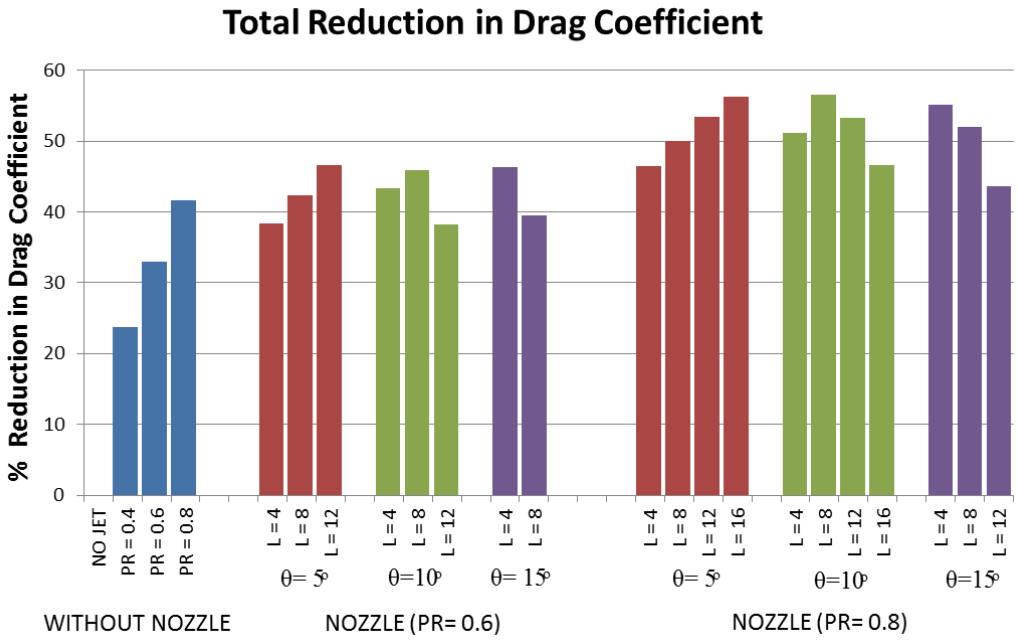

Figure 4-20 (%) Reduction in Drag Coefficient

CHAPTER 5

CONCLUSIONS & FUTURE WORK

5.1 Background

A brief summary of the work done and conclusive results obtained is presented. This effort marks only an initial step taken towards active drag reduction techniques. It opens windows of exploration in many directions both simple and complex to investigate many other aspects of this newly emerging technology. Recommendations in this regard also suggested in the literature to follow.

5.2 Conclusions

The current numerical effort was aimed at understanding the opposing jet concept initially, and ultimately introducing an effective technique for the better application of this newly emerging technology. After numerically validating the baseline experimental cases, a divergent nozzle of varying geometric configurations was introduced at the nose region of the same body. Two dimensional steady state simulations were conducted by varying both length and divergent angle of nozzle at three P.R. = 0.4, 0.6, 0.8 to reach an optimal nozzle + P.R. combination under the given flow conditions. A series of conclusions were reached which are mentioned as follows:

- A maximum of approximately 40 % drag reduction can be achieved at P.R = 0.8 without using any nozzle.

- With divergent nozzle the same reduction can be achieved at a lower pressure ratio 0.6. A maximum of 46 % drag reduction can be achieved [L4(15) case] .
- At P.R = 0.8 nozzle cases a maximum of 56 % drag reduction can be achieved [L8(10) case].
- For each pressure ratio a general trend can be noticed. At lower divergent angles the greater length provides a greater drag reduction. However at higher divergent angles the reverse phenomena occurs and greater lengths cause a decline in drag reduction.
- The use of a divergent nozzle is therefore recommended as it provides better results at lower pressure ratios.

5.3 Future Work

Based on the work done in this dissertation some recommendations for future research are as follows:

- In order to better understand LPM flow, the current analysis needs to be extended to transient simulations at lower pressure ratios. This is a complex and highly time dependent flow regime that may require three dimensional simulations.
- The effect of shock oscillations in LPM on the motion of body.
- The effect of jet ejection from nozzle at different angles of attack.
- The use of multiple jets (of varying size and positions) to see their effect on flow.
- Transient jet ejection from single and multiple jets.

BIBLIOGRAPHY

1. Anderson J. D., *Fundamentals of aerodynamics*.
2. Kral L. D., *Active Flow Control Technology.* ASME Fluids Engineering Division Technical Brief,
3. Manjunatha H. and Nataraj C. N., *Aerothermodynamic Design and Optimisation of Hypersonic Research Reentry Vehicle.* International Journal of Science and Research (IJSR), July 2014. Volume 3 Issue 7(2319-7064)
4. Ahmed M. Y. M. and N.Qin, *Recent advances in the aerothermodynamics of spiked hypersonic vehicles.* Progress in Aerospace Sciences, 2011(47(6):425-449).[doi:10.1016/j. paerosci.2011.06.001]
5. MARLEY C. D., *A Numerical Study Of Novel Drag Reduction Techniques For Blunt Bodies In Hypersonic Flows*. 2011, MISSOURI UNIVERSITY OF SCIENCE AND TECHNOLOGY.
6. Riggins D. W., Nelson H. F., and Johnson E., *Blunt body large wave drag reduction using focused energy deposition.* American Institute of Aeronautics and Astronautics Journal 37, 1998: p. pp.460-504
7. Knight D., *Survey of aerodynamic drag reduction at high speed by energy deposition.* Journal of Propulsion and Power, 2008(24(6):1153-1167).doi:10.2514/1.24595
8. Nair P., Jayachandran T., Deepu M. et al., *Numerical Simulation of Interaction of Sonic Jet with High Speed Flow over a Blunt Body using Solution Mapped Higher Order Accurate AUSM+-UP Based Flow Solver.* Journal of Applied Fluid Mechanics, 2010. Vol. 3, No. 1: p. pp. 15-23
9. Hayashi K., Aso S., and Tani Y., *Experimental Study on Thermal Protection System by Opposing Jet in Supersonic Flow.* Journal of Spacecraft and Rockets, 2006. 43(1): p. 233-235.10.2514/1.15332
10. *http://www.hitechweb.genezis.eu/*.
11. *http://www.thelivingmoon.com/*.
12. *http://www.aovi93.dsl.pipex.com/*.
13. Collins J. T., Meissinger H. F., and Bell R., *Small Orbit Transfer Vehicle (OTV) for On-Orbit Satellite Servicing and Resupply*, in *^15th Annual/USU Conference on Small Satellites*.
14. *nasa-crew-transfer-vehicle*
15. Hayashi K., Aso S., and Tani Y., *Numerical Study of Thermal Protection System by Opposing Jet.* 2005.10.2514/6.2005-188
16. Daso E. O., Pritchett V. E., Wang T.-S. et al., *Dynamics of Shock Dispersion and Interactions in Supersonic Freestreams with Counterflowing Jets.* AIAA Journal, 2009. 47(6): p. 1313-1326.10.2514/1.30084

17. Lopatoff M., *Wing-Flow Study Of Pressure -Drag Reduction At Transonic Speed By Projecting A Jet Of Air From The Nose Of A Prolate Spheroid Of Fineness Ratio 6.* NACA RESEARCH MEMORANDUM, Oct 1951(RM L51E09)
18. Love E. S., *The Effects of a Small Jet of Air Exhausting from theNose of a Body of Revolution in Supersonic Flow.* Nov. 1952. NACA RM L52I19a
19. Stadler J. R. and Inouye M., *A Method of Reducing Heat Transfer toBlunt Bodies by Air Injection.* May 1956. NACA RM A56B27a
20. Warren C. H. E., *An Experimental Investigation of the Effect of Ejectinga Coolant Gas at the Nose of a Bluff Body.* Journal of Fluid Mechanics, 1960. Vol. 8: p. pp. 400–417
21. Finley P. J., *The Flow of a Jet from a Body Opposing a Supersonic FreeStream.* Journal of Fluid Mechanics, 1966. Vol. 26: p. pp. 337–368
22. Rashis B., *Preliminary Indications of the Cooling Achieved byInjecting Water Upstream from the Stagnation Point of Hemispherical,80_ Conical, and Flat-Faced Nose Shapes at a Stagnation Temperatureof 4000 F.* Oct. 1957. NACA RM L57103
23. Barber E. A., *Experimental Investigation of Stagnation PointInjection.* Journal of Spacecraft and Rockets, 1965. Vol. 2(No. 5): p. pp. 770–774
24. Meyer B., Nelson H. F., and Riggins D. W., *Hypersonic Drag and Heat-Transfer Reduction Using a Forward-Facing Jet.* Journal of Aircraft, 2001. 38(4): p. 680-686.10.2514/2.2819
25. Hayashi K., Aso S., and Tani Y., *Numerical Study on Aerodynamic Heating Reduction by Opposing Jet.* March 2006. Memoirs of the Faculty of Engineering, Kyushu University, Vol.66, No.1
26. Jarvinen P. O. and Adams R. H., *The Effects of Retrorockets on the Aerodynamic Characteristics of Conical Aeroshell Planetary Entry Vehicles.* Jan. 1970. AIAA Paper 70-219
27. Hayashi K. and Aso S., *Effect of Pressure Ratio on Aerodynamic Heating Reduction due to Opposing Jet.* 2003.10.2514/6.2003-4041
28. Zheng Y. and Ahmed N., *A novel means of dissipation of shock wave induced heat in a high speed flow.* 2013.10.2514/6.2013-3114
29. Shah B. H. and Lu X.-Y., *Computational Study of Drag Reduction at Various Freestream Flows Using a Counterflow Jet from a Hemispherical Cylinder.* Engineering Applications of Computational Fluid Mechanics, 2014. 4(1): p. 150-163.10.1080/19942060.2010.11015306
30. Jarvinen P. and Adams R. H., *The Aerodynamic Characteristics Of Large Angled Cones With Retrorockets.* Feb 1970. NASA 7 - 576
31. Korzun A., Cordell J. C., and Braun R., *Comparison of Inviscid and Viscous Aerodynamic Predictions of Supersonic Retropropulsion Flowfields.* 2010.10.2514/6.2010-5048
32. Sriram R. and Jagadeesh G., *Film cooling at hypersonic Mach numbers using forward facing array of micro-jets.* International Journal of Heat and Mass Transfer, 2009. 52(15-16): p. 3654-3664. DOI 10.1016/j.ijheatmasstransfer.2009.02.035
33. Tamada I., Aso S., and Tani Y., *Reducing Aerodynamic Heating by the Opposing Jet in Supersonic and Hypersonic Flows.* 2010. AIAA. DOI 10.2514/6.2010-991

34. Morimoto N., Yoon J. Y., Aso S. et al., *Reduction of Aerodynamic Heating with Opposing Jet through Extended Nozzle in High Enthalpy Flow.* AIAA 2014. DOI 10.2514/6.2014-0705
35. Lu H. and Liu W., *Investigation of thermal protection system by forward-facing cavity and opposing jet combinatorial configuration.* Chinese Journal of Aeronautics, 2013. 26(2): p. 287-293.10.1016/j.cja.2013.02.005
36. Huang W., Yan L., Liu J. et al., *Drag and heat reduction mechanism in the combinational opposing jet and acoustic cavity concept for hypersonic vehicles.* Aerospace Science and Technology, 2015. 42: p. 407-414.10.1016/j.ast.2015.01.029
37. *http://www.asian-defence.net/2012/11/China-Developed-CM-400AKG-Pakistans-Hypersonic-Carrier-Killer-Missile-For-JF-17.html.*
38. *f9view.com/intercontinental-ballistic-missile-of-pakistan*.
39. *military.china.com*.
40. *www.suparco.gov.pk/.*
41. Zahir S., Asif M., Kamran N. et al., *Computational Investigations of aerodynamics forces at supersonic/Hypersonic Flows past a blunt body with various forward facing spikes.* AIAA- 2004-5189
42. Zaidi S. H., Shneider M. N., Mansfield D. K. et al., *Influence Of Upstream Pulsed Energy Deposition On A Shockwave Structure In Supersonic Flow* Aerodynamic Measurement Technology and Ground Testing Conference AIAA-2002-2703
43. Shah S. B. H. and Zahir S., *Numerical Simulation for the Comparative Investigations of a sonic Jet and Pin Protuberance in Supersonic Crossflow.* Proceedings of the 13th Asian Congress of Fluid Mechanics 17-21 December 2010, Dhaka, Bangladesh,
44. http://www.aerospaceweb.org/question/propulsion/q0220.shtml.
45. http://www.allstar.fiu.edu/aero/rocket3.htm.
46. Abdellah Hadjadj M. O., *Nozzle flow separation.* Springer 2009. Shock Waves (2009) 19: p. 163–169.DOI 10.1007/s00193-009-0209-7